© 2021. Published by The Company of Biologists Ltd | Journal of Cell Science (2021) 134, jcs247833. doi:10.1242/jcs.247833

RESEARCH ARTICLE

Tyrosine sulfation and O-glycosylation of chemoattractant receptor GPR15 differentially regulate interaction with GPR15L

Yukari Okamoto and Sojin Shikano

ABSTRACT

GPR15 is a G-protein-coupled receptor (GPCR) that directs lymphocyte homing to the colon and skin. Recent studies have identified a chemokine-like protein GPR15L (also known as C10orf99) as a functional ligand of GPR15. In this study, we examined the structural elements that regulate the GPR15–GPR15L interaction with primary focus on post-translational modifications (PTMs) of receptor N-terminus and on the C-terminus of the ligand. Our findings reveal that the GPR15 receptor is sulfated on the N-terminal tyrosine residue(s) and disruption of tyrosine sulfation inhibits binding of GPR15L. In contrast, the disruption of O-glycosylation on the N-terminal threonine or serine residues, or the removal of α2,3-linked sialic acids from O-glycans, enhances the GPR15L binding. Thus, GPR15 represents a unique chemoattractant receptor in which different N-terminal PTMs regulate its ligand binding in a contrasting manner. We further demonstrate that, unlike canonical chemokines, GPR15L activity critically requires its extreme C-terminal residue and that its hydrophobicity may be a key attribute that facilitates an optimal interaction with the receptor. Our results reveal novel insights into chemoattractant receptor–ligand interaction and provide a valid footing for potential intervention targeting the GPR15–GPR15L axis.

KEY WORDS: GPR15, GPR15L, C10orf99, Sulfation, O-glycosylation, Sialic acid

INTRODUCTION

GPR15 is a G-protein-coupled receptor (GPCR) family member that was initially identified as a co-receptor for the entry of the HIV-1, HIV-2 and simian immunodeficiency virus (SIV) (Deng et al., 1997). It is expressed in lymphoid tissues and in the colon. The discovery that GPR15 directs the migration of regulatory T cells to lamina propria in a mouse colon (Kim et al., 2013) has revealed a novel role of this receptor in the colon homing of T cells. Another extensive study by Nguyen et al. (Nguyen et al., 2015) demonstrated that GPR15 is also expressed by memory or effector T cells, and is responsible for inducing colitis in the mouse model that requires trafficking of these cells to the colon. A further study using a humanized mouse model of colitis also suggested a predominant role of GPR15 in the homing of human effector T cells to inflamed mucosa (Fischer et al., 2016). GPR15 also mediates the homing of dendritic epidermal T cells to the developing epidermis in fetal mice, plausibly contributing to the establishment of skin barrier function (Lahl et al., 2014). In addition, numerous recent studies have reported a strong correlation of chronic tobacco smoking and GPR15 expression in blood lymphocytes (Bauer et al., 2018; Kõks and Kõks, 2017), implying that this receptor could be involved in systemic inflammation.

GPR15L, a gene product of *C10orf99*, is a 57-amino-acid (mature form) polypeptide expressed in the colon (but poorly in small intestine), stomach, tonsil, skin and cervix in humans (Pan et al., 2014; Suply et al., 2017; Yang et al., 2015). C10orf99 (termed GPR15L hereafter) has been reported to have multifarious functions, including antimicrobial activity and cutaneous wound healing (Li et al., 2015; Yang et al., 2015). Moreover, it has been found to inhibit growth of colon cancer cells by binding to the transmembrane protein sushi domain-containing domain-2 (SUSD2) (Pan et al., 2014). More recent studies have discovered and established that GPR15L is a natural functional ligand of the GPR15 receptor. GPR15L exerts chemokine-like activities including the induction of Gαi-dependent inhibition of cAMP production, Ca^{2+} signaling, β-arrestin recruitment and *in vitro* migration of GPR15-expressing cells (Foster et al., 2019; Ocón et al., 2017; Suply et al., 2017). More importantly, unlike the canonical chemokine–receptor interaction, the GPR15–GPR15L interaction appears to be highly specific; GPR15L does not cross-activate any of the 22 chemokine receptors with known ligands, and the GPR15 receptor does not respond to any of the 27 known chemokines (Suply et al., 2017). Thus, the GPR15–GPR15L signaling axis represents a promising new therapeutic target for controlling the inflammation in the mucosal tissues, including the colon and the skin.

Earlier structure–function studies have substantiated the two-site/two-step binding model for chemokine ligand–receptor interaction, where the initial interaction with ligands occurs in the N-terminal tail of receptors and is followed by the formation of interactions with one or more extracellular loops (ECL) and/or the α-helical transmembrane (TM) segments (Rajagopalan and Rajarathnam, 2006). Although recent evidence now supports a more complex model (Kleist et al., 2016), functional roles of post-translational modifications (PTMs) of receptor N-terminal tail are well recognized (Stone et al., 2017). Many chemokine receptors are known to be sulfated on the tyrosine residues in the N-terminal tail and this tends to enhance chemokine binding to the receptor (Tan et al., 2013). GPR15 receptor has a cluster of tyrosine residues in the N-terminal tail that are the potential targets of sulfation. In addition, our previous study validated that GPR15 is O-glycosylated on the N-terminal threonine and/or serine residues (Okamoto and Shikano, 2011). However, whether and how these PTMs on GPR15 regulate the interaction with GPR15L have not been rigorously investigated. These seem particularly crucial questions since GPR15L, despite its chemokine-like functions, is distinct from canonical chemokine family proteins, such that it has no predictable preference for the formation of secondary structures such as β-strands and C-terminal helices (Suply et al., 2017). In addition, the binding mode of GPR15L

Department of Biochemistry and Molecular Genetics, University of Illinois at Chicago, Chicago, IL 60607-7170, USA.

*Author for correspondence (sshikano@uic.edu)

S.S., 0000-0003-0430-1284

Handling Editor: Daniel Billadeau
Received 17 April 2020; Accepted 15 March 2021

Journal of Cell Science (2021) 134, jcs247833. doi:10.1242/jcs.247833

to its receptor appears to be different from that of the majority of chemokines, which require their N-termini for receptor interaction and signaling (Loetscher and Clark-Lewis, 2001; Mizoue et al., 2001), since deletion of N-terminal 10 residues of GPR15L does not markedly influence Ca^{2+} flux by the GPR15 receptor (Suply et al., 2017). Instead, short C-terminal fragments of GPR15L by themselves are capable of activating the GPR15 receptor (Foster et al., 2019; Ocón et al., 2017; Suply et al., 2017), although the attributes of the C-terminal residues of GPR15L that contribute to the receptor binding are not known.

In this study, we investigated the biochemical nature of GPR15 modifications and the GPR15L C-terminal residue that regulates their interaction. Our results reveal that GPR15 is a unique chemoattractant receptor in which tyrosine sulfation and O-glycosylation/sialylation on the N-terminal tail differentially regulate the binding of its ligand, and that this binding appears to rely on the hydrophobicity of the extreme C-terminal residue of the ligand.

RESULTS

N-terminal FLAG-tagged GPR15L binds to the GPR15 receptor

To study the structural elements regulating the GPR15–GRP15L interaction, we first generated a recombinant GPR15L protein in HEK293T cells to measure equilibrium ligand binding to the receptor. GPR15L has been reported to be secreted as a 57-amino-acid mature polypeptide after cleavage of a 24-amino-acid signal peptide (Fig. 1A). We introduced a FLAG (DYKDDDDK) tag right after the signal peptide for detection and purification purposes. The culture supernatants from GPR15L-transfected cells were tested for whether the secreted FLAG–GPR15L bound specifically to the GPR15 receptor by flow cytometry (FCM)-based assay. Concentrations of GPR15L in the samples were determined by fluorescence-based western blotting using synthetic full-length GPR15L peptide [amino acids (aa) 1–57] as a standard (Fig. S1A). HEK293 cells transfected with vector or the GPR15 receptor were incubated at 4°C with culture supernatant from vector- or FLAG–GPR15L-transfected cells, followed by staining with phycoerythrin (PE)-conjugated anti-FLAG antibody (Ab). The left histogram in Fig. 1B illustrates a typical robust surface expression of the GPR15 receptor in HEK293 transfectants as determined with an anti-GPR15 Ab. The right histogram in Fig. 1B shows binding of FLAG–GPR15L to the GPR15-transfected but not the vector-transfected cells, indicating specific receptor–ligand interaction. By using the affinity-purified FLAG–GPR15L proteins, we observed a dose-dependent binding up to ∼1 µM (Fig. 1C; Fig. S1B) with a dissociation constant (K_D) of 172 nM, which is similar to the reported IC50 value of 100 nM previously determined with a ligand competition assay (Ocón et al., 2017). The FLAG–GPR15L in the culture supernatants used hereafter for the binding assays was adjusted to 75 nM by quantitative western blotting.

Tyrosine sulfation in GPR15 N-terminal tail contributes to binding of GPR15L

Chemokine receptors often undergo PTMs in the N-terminal extracellular domain (Szpakowska et al., 2012). We addressed whether the PTMs of the GPR15 receptor impacted its interaction with GPR15L. One of the receptor modifications that are known to promote chemokine binding is tyrosine sulfation, which was first demonstrated in the N-terminal tail of CCR5. The binding of cognate ligands CCL3 and CCL4, and HIV-1 gp120 protein to CCR5 was decreased by sulfation inhibitor treatment or mutation of the N-terminal tyrosine residues (Farzan et al., 1999). Since this finding, various chemokine receptors have been found to require N-terminal sulfation for the optimal binding of their ligands (Tan et al., 2013). The N-terminus of GPR15 entails four tyrosine residues (Fig. 2A, red) adjacent to the acidic residue, a key feature of tyrosine sulfation (Bundgaard et al., 1997). To see whether GPR15 is modified by tyrosine sulfation, we generated a Myc-tagged GPR15 tyrosine to phenylalanine mutant (hereafter denoted Y/F mutant GPR15) in which all four tyrosine residues were replaced by phenylalanine residues. As we reported previously (Okamoto and Shikano, 2011), when transiently expressed in HEK293 cells, the wild-type GPR15 is partially O-glycosylated, as represented by a slower migrating form (Fig. 2B, marked by *) and this form primarily represents the surface-expressed population. The Y/F mutant GPR15 exhibited increased electrophoretic mobility in the western blot (Fig. 2B), most likely due to the alterations in SDS binding, as reported in the other studies on the GPCRs with a tyrosine to phenylalanine mutation (Farzan et al., 1999; Gao et al., 2003). The cells expressing Myc-tagged wild-type (WT) or Y/F mutant GPR15 were labeled with sodium [^{35}S]sulfate in the presence or absence of a sulfation inhibitor sodium chlorate, and the GPR15 proteins were immunoprecipitated by anti-Myc Ab. The eluants were subjected to ^{35}S autoradiography (left panel), followed by immunoblotting with anti-Myc Ab (right panel). A strong signal of ^{35}S in the eluant of GPR15 WT and markedly reduced signal in both Y/F mutant and sodium chlorate-treated WT (Fig. 2C, left panel, marked by *) strongly suggested that GPR15 is sulfated and

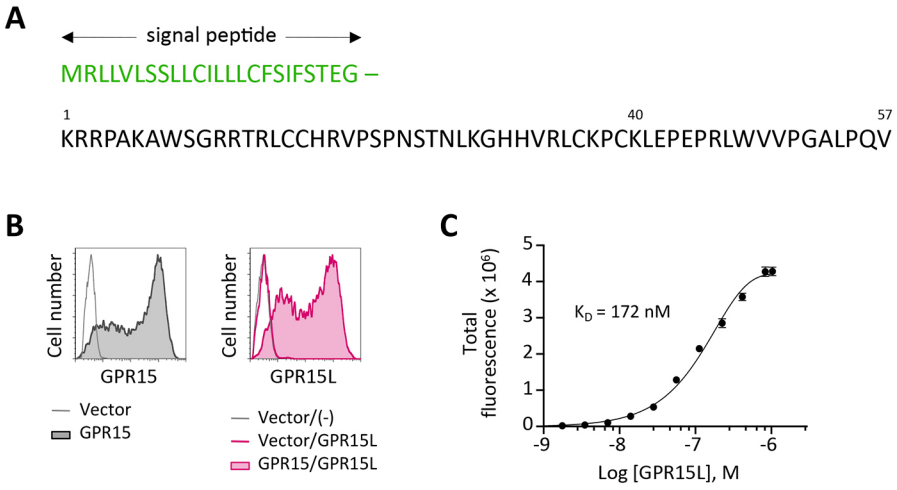

Fig. 1. N-terminal FLAG-tagged GPR15L binds to the GPR15 receptor. (A) Amino acid sequence of GPR15L (C10orf99) in humans. Amino acid numbers 1–57 are assigned to the mature protein downstream of a signal sequence (green). (B) Surface expression of GPR15 and binding of FLAG-GPR15L. HEK293 cells transfected with vector or untagged GPR15 were stained for surface GPR15 with anti-GPR15 Ab followed by AF488-secondary Ab (left panel) or examined for the ligand binding by incubation with culture supernatant containing 75 nM FLAG-GPR15L followed by PE-FLAG Ab (right panel). (C) Dose-dependent receptor binding of purified FLAG–GPR15L in the transfected HEK293 cells. The K_D value was determined by Prism software (GraphPad). Results representative of three experiments.

Journal of Cell Science (2021) 134, jcs247833. doi:10.1242/jcs.247833

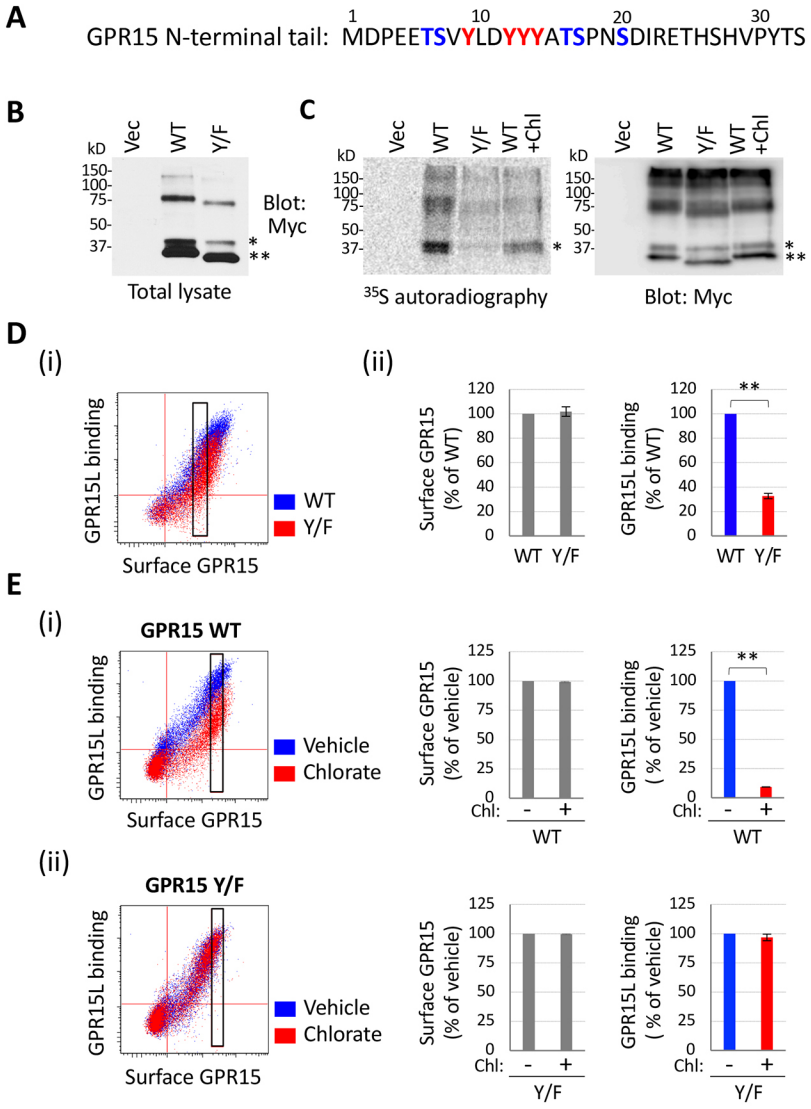

Fig. 2. Tyrosine sulfation in GPR15 N-terminal tail contributes to binding of GPR15L. (A) Amino acid sequence of the human GPR15 N-terminal tail (aa 1–33). Tyrosine, and threonine and serine residues that are mutated in this study are highlighted in red and blue, respectively. (B) Myc-tagged GPR15 WT or Y/F mutant with all four tyrosine residues replaced by phenylalanine resides were expressed in HEK293 cells and blotted for Myc. The upper (*) and lower (**) bands represent the mature (O-glycosylated) and immature (unglycosylated) form of monomeric GPR15, respectively. The larger molecular mass bands of ~75 kDa are the dimeric forms. (C) [^{35}S]sulfate labeling of GPR15. The cells transfected with vector or Myc–GPR15 were incubated overnight with sodium [^{35}S]sulfate in the presence or absence of the sulfation inhibitor sodium chlorate. The immunoprecipitated Myc–GPR15 proteins were sequentially analyzed by autoradiography (left panel) and then by Myc blotting (right panel). Note that the mobility of radioactive bands marked by * matches that of the O-glycosylated mature bands * of the Myc blot. The faster migrating bands marked by ** are the unglycosylated forms. Results in B and C representative of two experiments. (D) Binding of FLAG–GPR15L to the Y/F mutant receptor. (i) Myc–GPR15-transfected cells were incubated with FLAG–GPR15L-containing supernatant and then double stained with AF488–Myc and PE–FLAG Abs. Illustrated here is a representative dot plot of three replicates for double-stained cells in which the thresholds of Myc and FLAG signals are depicted with red lines. The gated cell populations (black rectangle) were quantified for surface Myc–GPR15 expression (ii, left panel) and FLAG-GPR15L binding (ii, right panel). (E) Effect of a sulfation inhibitor on the GPR15L binding. Cells transfected with (i) WT or (ii) Y/F mutant GPR15 were treated with vehicle or sodium chlorate for 24 h and subjected to Myc staining and FLAG–GPR15L binding. The gated cell populations (black rectangle) in the left panels were quantified for Myc–GPR15 (middle panels) and FLAG-GPR15L (right panels). Quantitative results are mean±s.e.m. (n=3). **P≤0.01 (Student's t-test).

that this occurs primarily on at least one of the N-terminal tyrosine residues. The electrophoretic mobility of the radioactive bands matched those of the mature (O-glycosylated) bands (Fig. 2C, right panel, marked by *), consistent with the notion that both tyrosine sulfation and O-glycosylation occur only on the receptors that have reached the Golgi.

At this stage, we tested whetehr tyrosine sulfation affected the ligand binding to GPR15. HEK293 cells transfected with Myc–GPR15 WT or Y/F mutant were incubated with FLAG–GPR15L and then stained simultaneously with Alexa Fluor 488 (AF488)-labeled anti-Myc and PE-labeled anti-FLAG to measure the surface GPR15 level and the GPR15L binding, respectively. Since Y/F mutant GPR15 showed an overall lower level of surface expression in comparison with WT GPR15 when transfected into HEK293 cells, we focused on the cell populations (gate in Fig. 2Di) that are expressing equivalent levels of surface GPR15 (Fig. 2Dii, left panel) for analyzing the ligand binding. In those gated cells, GPR15L binding to Y/F mutant receptor was significantly lower than that of the WT receptor (Fig. 2Dii, right panel). This was not caused by the Myc-tagging of the GPR15 receptor, because we also observed considerably reduced ligand binding to the Y/F mutant of the untagged GPR15 receptor expressed in HEK293 cells (Fig. S2A). To confirm that the reduced binding of GPR15L to Y/F receptor is due to the loss of sulfation rather than the effect of amino acid substitution per se, we treated cells with sodium chlorate, a sulfation inhibitor, and examined for the ligand binding. When analyzed for the cell populations showing an equivalent level of surface receptor expression (Fig. 2Ei, left and middle panels), the WT receptor-expressing cells treated with sodium chlorate showed significantly reduced binding of GPR15L (Fig. 2Ei, right panel). In contrast, GPR15L binding to the Y/F mutant receptor was not affected by sodium chlorate treatment (Fig. 2Eii, right panel) when analyzed for those at the equivalent level of surface expression (Fig. 2Eii, left and middle panels), strongly indicating that the effect of sodium chlorate on ligand binding is due to the altered sulfation on the tyrosine residues of GPR15. Altogether, our results demonstrate that sulfation on the N-terminal tyrosine residue(s) of GPR15 is imperative for the optimal binding of GPR15L.

Sulfated peptide fragments from N-terminal tail of several chemokine receptors have been shown to bind their cognate ligands *in vitro* (Seibert et al., 2008; Zhu et al., 2011). We examined whether the GPR15 N-terminal tail by itself is sufficient to establish binding of ligand on the cell surface by using a chimeric receptor consisting of the GPR15 N-terminal tail and the rest of the regions from another chemokine receptor, CXCR4. This chimeric receptor displayed robust surface expression that was comparable to the WT

Journal of Cell Science (2021) 134, jcs247833. doi:10.1242/jcs.247833

GPR15 as detected by the anti-GPR15 Ab, but showed no detectable binding of FLAG-GPR15L (Fig. S3). Thus, it can be deduced that the N-terminal tail of GPR15 by itself is not sufficient to establish a stable binding of GPR15L on the cell surface and other receptor domains are critically required as well.

Sialylated O-glycans in the GPR15 N-terminal tail inhibits binding of GPR15L

Human GPR15 has no consensus N-glycosylation sites (Asn-X-Thr/Ser) in any of its extracellular domains. Instead, we previously reported that GPR15 is O-glycosylated on at least one of the threonine or serine residues in the N-terminal tail (aa 6, 7, 16, 17, and 20; Fig. 2A, shown in blue) (Okamoto and Shikano, 2011). In comparison with N-glycosylation, which is known to be important for biogenesis and signaling in many GPCRs (Nørskov-Lauritsen et al., 2015), the presence and/or the functional role of O-glycosylation in GPCRs have been affirmed for a very limited number of receptors (Bannert et al., 2001; Gutiérrez et al., 2004; Petäjä-Repo et al., 2000; Sadeghi and Birnbaumer, 1999). For CCR5 and CCR8, the O-glycosylation on the N-terminal threonine and serine residues has been shown to promote ligand binding (Farzan et al., 1999; Gutiérrez et al., 2004). In this study, we addressed the role of O-glycosylation in the ligand binding of GPR15. First, we compared the cells expressing the WT and TS/AA mutant receptor in which five N-terminal threonine and serine residues were replaced by alanine residues. The TS/AA mutant lacks the slower migrating band, indicating a loss of O-glycosylation (Okamoto and Shikano, 2011; and Fig. 3Ai, marked by *). These transfected cells were examined for the binding of FLAG–GPR15L. Since the TS/AA mutant showed overall lower surface expression than WT upon transient transfection, we again focused on the cells that express an equivalent level of surface GPR15 (Fig. 3Aii, left and middle panels) to analyze for the ligand binding. The TS/AA mutant in the gated cells showed ∼7-fold higher binding of FLAG–GPR15L than the WT receptor (Fig. 3Aii, right panel). These data suggested that the O-glycans on the GPR15 N-terminal tail inhibit the binding of GPR15L. The enhanced ligand binding by TS/AA mutation was also confirmed with an untagged GPR15 receptor (Fig. S2B).

Since the replacement of the N-terminal threonine and serine residues for alanine not only disrupts O-glycosylation but may potentially alter the local conformation of the polypeptides and possibly affect ligand binding, we used ldlD mutant Chinese hamster ovary (CHO) cells to address the role of O-glycans without amino acid substitution. The ldlD cells lack the UDP-galactose/UDP-N-acetylgalactosamine (GalNAc) 4-epimerase and therefore are deficient in GalNAc O-glycosylation and galactosylation in the

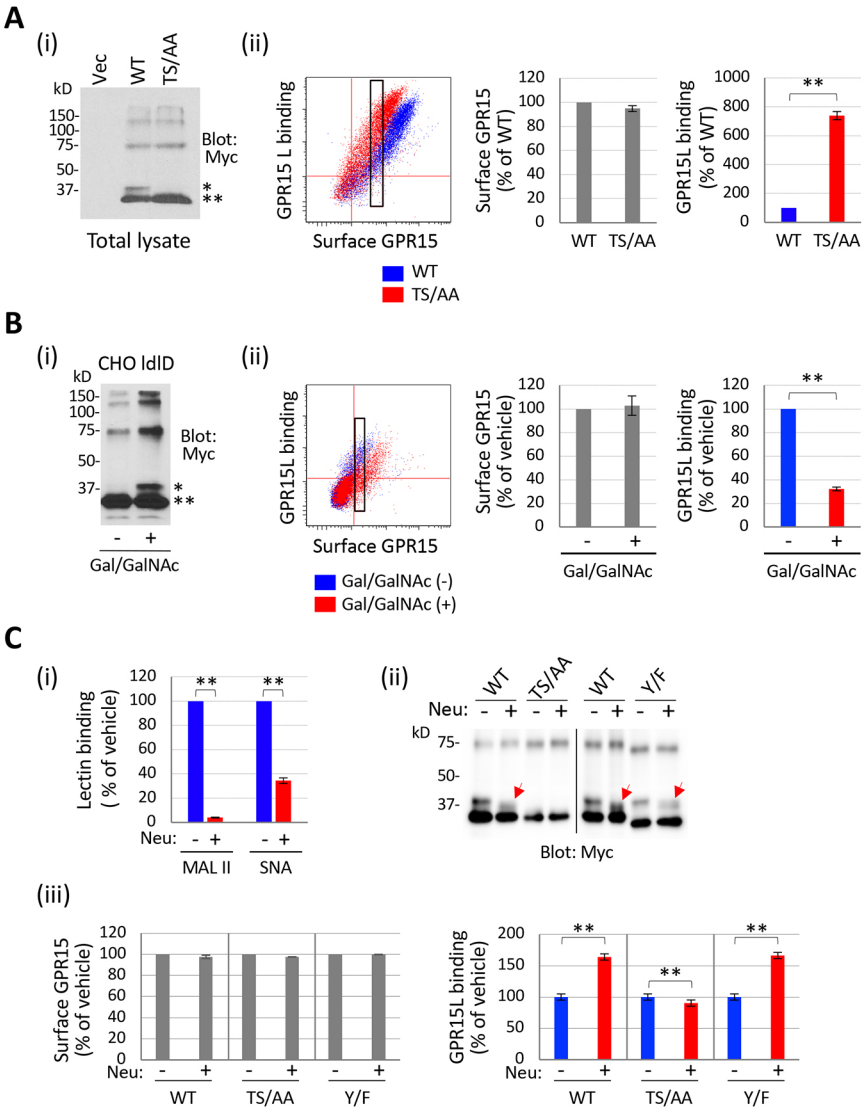

Fig. 3. O-glycosylation in GPR15 N-terminal tail inhibits binding of GPR15L. (A) GPR15L binding to the O-glycosylation-deficient GPR15 receptor. (i) WT and mutant Myc-GPR15 receptor with five threonine and serine residues replaced by alanine (TS/AA) were immunoblotted for Myc. The TS/AA mutant lacks the O-glycosylated form (*) and shows only the unglycosylated form (**). (ii) Binding of FLAG–GPR15L to the TS/AA mutant receptor. The cells transfected with the WT or TS/AA mutant Myc–GPR15 were subjected to FLAG–GPR15L binding and Myc staining. The gated cell populations (left panel, black rectangle) were quantified for Myc–GPR15 signal (middle panel) and FLAG–GPR15L signal (right panel). (B) FLAG–GPR15L binding in the O-glycosylation-deficient CHO cell. (i) CHO ldlD cells transfected with Myc–GPR15 WT were cultured overnight with vehicle or galactose (Gal) and N-acetylgalactosamine (GalNAc), and then cell lysates were immunoblotted for Myc. The cells treated with sugars show both glycosylated (*) and unglycosylated (**) forms of GPR15. (ii) Myc–GPR15-transfected ldlD cells treated with or without Gal and GalNAc were subjected to FLAG–GPR15L binding assay and Myc staining. The gated cell populations (left panel, black rectangle) were quantified for Myc–GPR15 signal (middle panel) and FLAG–GPR15L signal (right panel). (C) FLAG–GPR15L binding to sialic acid-removed GPR15 receptor. (i) GPR15-transfected HEK293 cells were treated or not with neuraminidase from *A. ureafaciens* and then incubated with biotin–MALII or biotin–SNA, followed by PE–streptavidin. (ii) The Myc–GPR15-transfected HEK293 cells were treated or not with neuraminidase as above and cell lysates were immunoblotted for Myc. Note the mobility shift of the O-glycosylated form (arrows) caused by neuraminidase treatment, suggesting removal of sialic acids. (iii) The cells treated or not with neuraminidase as described above were subjected to FLAG–GPR15L binding and Myc staining. The gated cell populations (not shown) were quantified for Myc–GPR15 (left panel) and FLAG–GPR15L signals (right panel). Quantitative results are mean±s.e.m. (n=3). Blots and FCM images shown are representative of three experiments. **$P\leq0.01$ (Student's t-test).

Journal of Cell Science (2021) 134, jcs247833. doi:10.1242/jcs.247833

absence of exogeneously-added GalNAc and galactose, respectively (Kingsley and Krieger, 1984). The appearance of a slower migrating mature form (marked by *) in the presence of GalNAc and galactose confirms O-glycosylation of GPR15 in this cell (Fig. 3Bi and Okamoto and Shikano, 2011). Even though the surface expression level of GPR15 was observed to be slightly higher for the cells cultured with sugars (Fig. 3Bii, left and middle panels), those cells showed more than three times lower binding of FLAG–GPR15L than the cells cultured without sugars (Fig. 3Bii, right panel). Altogether, these results corroborate the notion that O-glycans on the N-terminal threonine and serine residues of GPR15 inhibit the binding of GPR15L. Thus, GPR15 represents the first chemoattractant receptor in which tyrosine sulfation and O-glycosylation in the N-terminal tail opposingly regulate the binding of a ligand.

Carbohydrate chains are typically capped with sialic acids (Byrne et al., 2007). For CCR5 and CCR8, the removal of sialic acids by neuraminidase treatment of cells results in the loss of ligand binding (Bannert et al., 2001; Gutiérrez et al., 2004). We addressed the potential role of sialic acids in the GPR15–GPR15L interaction by treating cells with neuraminidase from *Arthrobacter ureafaciens*. This neuraminidase removed both α2,3- and α2,6-linked sialic acids on HEK293 cells, as indicated by the reduced cell surface binding of sialic acid-binding lectins MALII and SNA, which are specific for α2,3- and α2,6-linked sialic acid, respectively (Fig. 3Ci). The neuraminidase treatment of cells resulted in the mobility shift of the O-glycosylated form of WT GPR15 (Fig. 3Cii, arrow) but not the unglycosylated forms of WT and TS/AA, indicative of sialylation (Gahmberg and Andersson, 1982). When the cell populations with an equivalent level of surface GPR15 expression (Fig. 3Ciii, left panel) were analyzed for the FLAG–GPR15L binding, the WT GPR15-expressing cells showed ∼1.7-fold higher binding of ligand upon neuraminidase treatment (Fig. 3Ciii, right panel). In contrast, neuraminidase treatment did not increase ligand binding in the cells expressing the TS/AA mutant GPR15 (Fig. 3Ciii, right panel). These results suggest that the enhanced ligand binding to the neuraminidase-treated cells expressing WT GPR15 is caused by the loss of sialic acids on the N-terminal threonine and serine residues. Thus, sialic acids on the N-terminal O-glycans are at least partly responsible for the inhibition of GPR15L binding to the receptor.

It is conceivable that the sialylated O-glycans block GPR15L binding by preventing the ligand from accessing the neighboring sulfated tyrosine residues. We addressed this possibility by gauging the effect of neuraminidase on ligand binding to the Y/F mutant GPR15 receptor, which lacks the N-terminal tyrosine residues but still appears to be sialylated, as judged by the mobility shift of glycosylated band upon neuraminidase treatment (Fig. 3Cii, right-hand two lanes, arrow). The neuraminidase treatment of Y/F mutant-expressing cells led to the noticeably increased binding of GPR15L (Fig. 3Ciii, right panel), similar to the WT receptor. This indicates that the removal of sialic acids from O-glycans allows a stronger binding of GPR15L even in the absence of sulfated tyrosine, implying that sialylated O-glycans prevent GPR15L binding irrespective of the sulfation of tyrosine residues.

PTM of GPR15 regulates GPR15L-induced receptor signaling

Having differential regulatory roles of tyrosine sulfation and O-glycosylation in ligand binding, we attempted to ascertain whether these PTMs impact the ligand-induced signaling of GPR15. To accomplish this goal, we performed an ERK1 and ERK2 (ERK1/2; also known as MAPK3 and MAPK1, respectively) activation assay using fluorescence-based western blotting. Fig. 4A depicts that synthetic full-length GPR15L (aa 1–57) induces ERK1/2 phosphorylation in a dose-dependent manner up to 200 nM in HEK293 cells transfected with WT GPR15 (Fig. 4A, left-most panel). Since the C-terminal domain of GPR15L alone is known to be capable of activating GPR15 (Foster et al., 2019; Ocón et al., 2017; Suply et al., 2017), in this study, we also examined the C-terminal fragments of GPR15L encoding the last 18, 13 and 11 residues, which contain different numbers of charged residues, to address whether receptor activation by these fragments is also regulated by the receptor PTM. These fragment peptides dose-dependently activated ERK1/2 (Fig. 4A, right-most three panels) although with substantially lower efficiency than that of full-length GPR15L, which is consistent with results from previous studies reporting an ∼100 times lower capacity of the C-terminal fragments in GPR15 signaling (Foster et al., 2019; Suply et al., 2017).

We tested whether the Y/F or TS/AA mutation of the GPR15 receptor affects the ligand-induced ERK1/2 activation. Since the transient transfection of Y/F or TS/AA mutant GPR15 in HEK293 cells results in lower surface expression than the WT receptor and the ERK assay measures the total signal from the entire cell population, we used a reduced amount (1/4) of WT plasmid to attain similar levels of surface expression. Fig. 4B shows the surface expression levels of GPR15 in the cells used for these ERK activation assays, where WT and Y/F were similar while the TS/AA mutant still showed a lower level. Under this transfection condition, we found that ERK1/2 activation by full-length GPR15L was significantly reduced in Y/F mutant-expressing cells while it was enhanced in the TS/AA mutant-expressing cells (Fig. 4C,D, GPR15L lanes). This is consistent with the binding pattern of FLAG–GPR15L to these mutant receptors (Figs 2 and 3), suggesting that tyrosine sulfation and O-glycosylation of GPR15 regulate ligand-induced signaling by modulating the binding efficacy of GPR15L. Interestingly, we found that ERK1/2 activation by the C-terminal 18-, 13-, and 11-mer fragments was also regulated by the Y/F and TS/AA mutations to a similar level to that by full-length GPR15L (Fig. 4C,D). This raises a possibility that tyrosine sulfation and O-glycosylation impact GPR15 signaling at least partly by regulating the interaction of the ligand C-terminal domain with the receptor.

Tyrosine sulfation and sialylation regulate GPR15L binding in T cells

Since types and abundances of protein PTMs are anticipated to vary between different cell types (Goh and Ng, 2018), we addressed whether tyrosine sulfation and sialylation of GPR15 also regulate GPR15L binding in the cell context in which GPR15 is endogenously expressed. We used the T cell lymphoma line HuT 78, for which we previously demonstrated detectable expression of GPR15 on the plasma membrane (Okamoto and Shikano, 2017). Since the surface expression level of endogenous GPR15 was insufficient to facilitate reliable binding of FLAG-tagged GPR15L (data not shown), we stably transfected HuT 78 cells with an untagged GPR15 gene to increase its surface expression (Fig. 5A). In western blots, the anti-GPR15 C-terminus Ab detected a diffused band signal in HuT 78 cells that were enhanced by GPR15 transfection (Fig. 5B, marked by **) and migrated slower than those in GPR15-transfected HEK293 cells (Fig. 5B, marked by *), suggesting a difference in PTMs. Using this GPR15-transfected HuT 78 cells, we first tested whether tyrosine sulfation plays a role in the GPR15L binding. Treatment of cells with 0.5 mM sodium chlorate, which did not significantly alter the surface level of GPR15 (Fig. 5C, left panel), resulted in significantly lower binding of FLAG–GPR15L (Fig. 5C, right panel). This suggests that tyrosine sulfation of GPR15 also contributes to the interaction with GPR15L in a T cell context.

Journal of Cell Science (2021) 134, jcs247833. doi:10.1242/jcs.247833

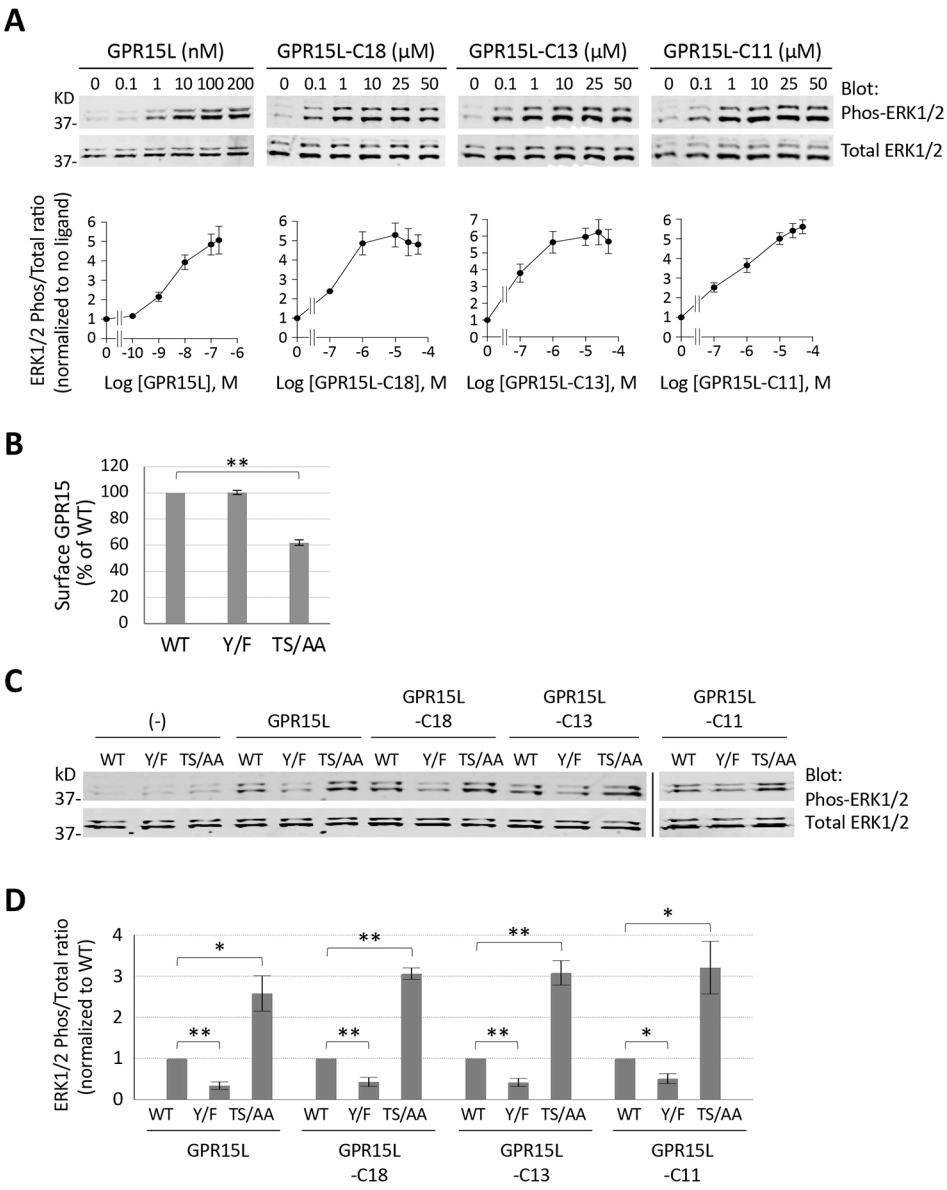

Fig. 4. PTM of GPR15 regulates GPR15L-induced receptor signaling. (A) Dose-dependent ERK1/2 activation by GPR15L and C-terminal fragments of GPR15. HEK293 cells transfected with Myc–GPR15 were incubated with the indicated amounts of synthetic full-length GPR15L peptide or C-terminal 18-mer (C-18), 13-mer (C-13) or 11-mer (C-11) peptide and the cell lysates were analyzed for phosphorylated and total ERK1/2 (upper panels). Ratios of phosphorylated ERK to total ERK from ligand-treated samples were normalized with respect to that from no-ligand sample (lower panels). (B) Effects of disruption of tyrosine sulfation and O-glycosylation on GPR15L-induced ERK1/2 activation. Cells were transfected with WT (1/4 amount of Y/F and TS/AA plasmid), Y/F or TS/AA mutant Myc–GPR15 and a portion of cells used for the ERK1/2 assays were subjected to surface Myc staining to determine surface expression of GPR15. The graph shows the Myc signal for the entire cell populations. (C) HEK293 cells transfected as described in B were stimulated with full-length GPR15L (100 nM) or C-terminal fragment (10 μM) and the lysates were analyzed for the ERK1/2 activation. (D) Data are shown as the ratio of phospho-ERK1/2 to total ERK1/2 band intensities and further normalized to those of WT. Quantitative results are mean±s.e.m. (n=3). Blots shown are representative of three experiments. *P≤0.05; **P≤0.01 (Student's t-test).

Next, we addressed whether GPR15 is sialylated in HuT 78 and whether that regulates the binding of GPR15L. Here, we used a neuraminidase from *Vibrio cholerae* at a concentration that substantially (>90%) reduced the binding of MALII but not SNA to HuT 78 cells (Fig. 5D) to ensure preferential digestion of α2,3- but not α2,6-linked sialic acids. We immunoprecipitated GPR15 proteins from HuT 78 cells that were treated or not with this neuraminidase, and examined for sialylation by means of a lectin blot. The neuraminidase treatment caused a discernible mobility shift of GPR15 in the anti-GPR15 blot (Fig. 5E, left panel), suggesting sialylation. In essence, the MALII blot of GPR15 immunoprecipitant detected a band signal at a position that matches a slower-migrating GPR15 band and this was abolished by the neuraminidase treatment (Fig. 5E, right panel). We also conducted blotting with SNA but failed to detect any band signals specific to the GPR15 immunoprecipitant (data not shown). Under this neuraminidase treatment condition, we next performed a ligand-binding assay using FLAG–GPR15L. The neuraminidase treatment of HuT 78 cells did not significantly change the surface expression of the GPR15 receptor (Fig. 5F, left panel), rather resulted in the significantly increased binding of FLAG–GPR15L (Fig. 5F, right panel), consistent with the results in HEK293 transfectants. On the whole, our results demonstrate that the GPR15 receptor is at least α2,3-sialylated in the T cell context and that these sialic acids negatively regulate the binding of the GPR15 ligand.

The extreme C-terminal residue of GPR15L is required for receptor binding

Having the information that the C-terminal fragment of GPR15L alone can activate the receptor (Fig. 4A), we next addressed the role of the extreme C-terminal residues of GPR15L in receptor binding by testing the truncation mutants. We used C-terminally truncated FLAG–GPR15L mutants expressed in the culture supernatant at similar levels, as determined by a FLAG blot (Fig. 6Ai). We found that the C-terminal deletion of even one residue (Δ56) significantly reduced binding and further truncation up to aa 54 (Δ54) almost completely abolished the binding (Fig. 6Aii). To address the functional role of C-terminal residues in receptor signaling, we stimulated the GPR15-expressing cells with the WT or Δ54 mutant GPR15L and examined for the ERK1/2 activation. Consistent with

Journal of Cell Science (2021) 134, jcs247833. doi:10.1242/jcs.247833

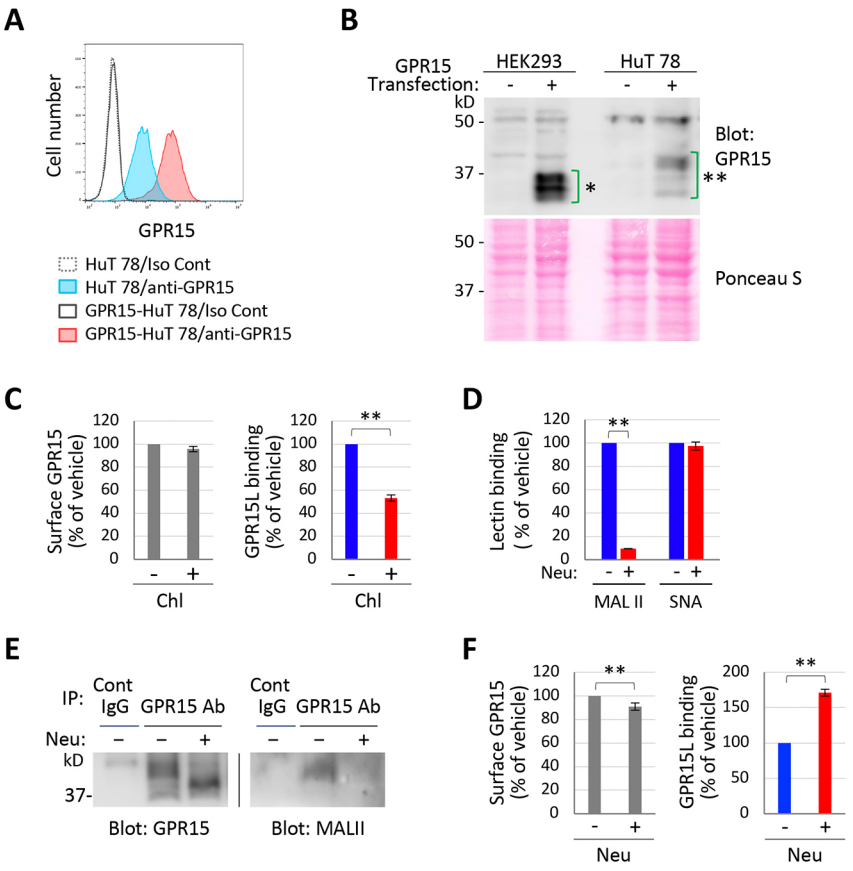

Fig. 5. Sialylation of GPR15 inhibits GPR15L binding in lymphoma T cell line. (A) Surface expression of GPR15 in HuT 78 cells. Cells with or without retroviral transfection of untagged GPR15 were stained with anti-GPR15 or isotype Ab followed by secondary Ab. (B) Untagged GPR15 proteins in transiently transfected HEK293 and retrovirally transfected HuT 78 cells were probed with anti-GPR15 C-terminus Ab. Band signals that are enhanced by GPR15 transfection in HEK293 and HuT 78 are marked by (*) and (**), respectively. The lower panel is a Ponceau S staining of the transfer membrane. Hereafter, the term 'HuT 78' refers to the HuT 78 cells that were retrovirally transfected with GPR15. Results in A and B are representative of three experiments. (C) Effect of a sulfation inhibitor on GPR15L binding to HuT 78 cell. The cells were treated overnight with sodium chlorate and then examined for surface expression of GPR15 (left panel) and FLAG–GPR15L binding (right panel). (D) Effect of neuraminidase on the cell surface sialic acids of HuT 78 cells. The cells were treated or not with neuraminidase from *V. cholerae* and then incubated with biotin–MALII or biotin–SNA, followed by PE–streptavidin. (E) Sialylation of GPR15 in HuT 78 cell. The GPR15 proteins were immunoprecipitated from HuT 78 cells treated or not with neuraminidase and then blotted with anti-GPR15 Ab and HRP-secondary Ab (left panel) or with biotin–MALII and HRP-streptavidin (right panel), followed by chemiluminescence analysis. Images representative of three experiments. (F) Effect of desialylation on GPR15L binding in HuT 78 cell. The cells treated or not with neuraminidase were examined for the surface GPR15 (left panel) and binding of FLAG-GPR15L (right panel). Quantitative results are mean±s.e.m. (n=3). **P≤0.01 (Student's t-test).

their receptor binding profile, Δ54 showed only a background level of ERK1/2 phosphorylation (Fig. 6B). These data demonstrate that the C-terminal residues of GPR15L are critically involved in the binding to and activation of the GPR15 receptor.

Hydrophobicity of the extreme C-terminal residue of GPR15L is important for receptor binding and activation

GPR15L in most of the vertebrates has a valine residue at the extreme C-terminus with exceptions of isoleucine (in mouse and rat) and methionine (in mole-rat and armadillo) (Ocón et al., 2017; Suply et al., 2017). A mutagenesis analysis was performed to determine the attributes of the extreme C-terminal residue contributing to the receptor binding. The C-terminal valine was replaced with 13 different amino acids, and the supernatants containing these mutant ligands were examined for the binding capacity to the GPR15 receptor. Fig. S4A depicts a representative FLAG blot of the culture supernatants used for the binding assay showing that they exhibited similar levels of GPR15L except for alanine, methionine and

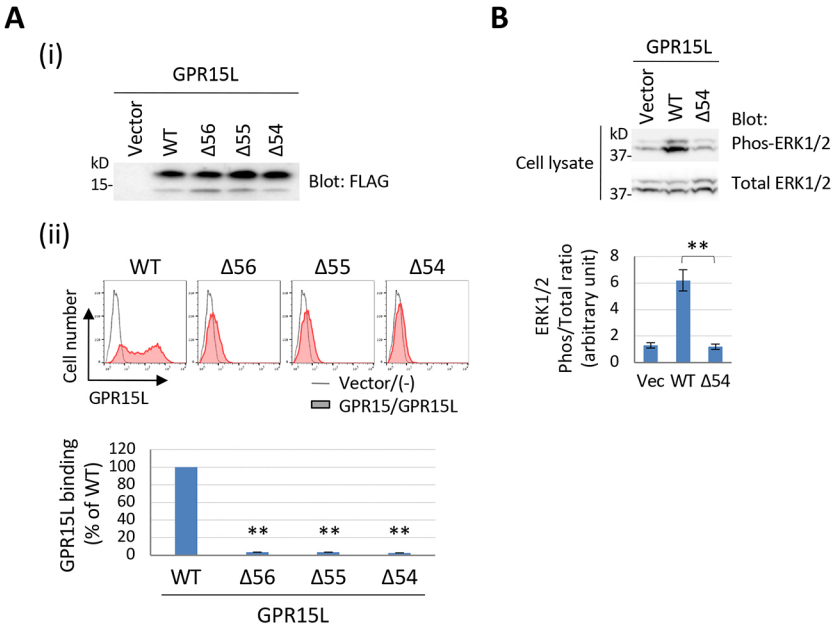

Fig. 6. The extreme C-terminal residue of GPR15L is required for receptor binding. (A)(i) Expression of C-terminally truncated FLAG–GPR15L. Culture supernatants from WT- and truncated FLAG–GPR15L-transfected cells were blotted for FLAG. The two bands with different migration speed represent the protein modification related to the glycosylation (our unpublished data). Images representative of three experiments. (ii) HEK293 cells transfected with WT GPR15 receptor were subjected to FLAG–GPR15L binding using the culture supernatants shown in i. The upper panels show representative histograms of three experiments. The open area represents vector-transfected cells stained with PE–FLAG Ab, and the filled area is from GPR15-transfected cells incubated with FLAG–GPR15L followed by PE–FLAG Ab. The lower panel is a quantification of the FLAG–GPR15L binding signals. (B) ERK1/2 activation by C-terminally truncated GPR15L. HEK293 cells transfected with WT GPR15 were stimulated with culture supernatants containing WT and Δ54 FLAG-GPR15L and cell lysates were analyzed for the ERK1/2 activation. Blot representative of three experiments. Quantitative results are mean±s.e.m. (n=3). **P≤0.01 (Student's t-test).

Journal of Cell Science (2021) 134, jcs247833. doi:10.1242/jcs.247833

arginine, which contained slightly higher amounts. The receptor binding assay using those FLAG–GPR15L revealed that the hydrophobic residues including phenylalanine, isoleucine, leucine, tryptophan and tyrosine at aa 57 enabled comparable or even higher binding of GPR15L than valine, ranging between 95–159% (Fig. 7A). Met was fairly less effective but still supported the binding at 79% of valine. Other less or not hydrophobic residues we tested (Ala, Asp, Lys, Pro and Arg) were considerably less effective in supporting the binding (8%–27% of Val), with the only exception of Ser which conferred 54% binding of valine. The replacement with cysteine resulted in an extremely poor expression of the ligand protein and thus was not examined (data not shown). These results suggest that the hydrophobicity of the extreme C-terminal residue is pivotal for the optimal binding of GPR15L to the receptor. However, the fact that tyrosine, which is generally not regarded as the most hydrophobic amino acid, showed the highest binding suggests that other attributes of the aa 57 may potentially contribute to the receptor binding of GPR15L.

To assess whether the observed differences in the binding capacity of the C-terminal mutants impact GPR15 receptor signaling, we selected V57Y, which showed the highest binding among the hydrophobic ligands, and V57A, which is less hydrophobic and showed lower binding than WT, to compare with WT ligand for their capacity to activate ERK1/2. FLAG-tagged GPR15L proteins (WT, V57, and V57A) were obtained at adequately high purity as determined by Coomassie Brilliant Blue-stained SDS-PAGE gels (Fig. S4B). The V57Y mutant ligand induced ERK1/2 activation at a lower dose than WT did, while the V57A mutant required a higher dose for receptor activation than WT (Fig. 7B). We also performed the ERK activation assay using the synthetic C-terminal 18-mer peptides of WT, V57Y and V57A ligands. We observed a similar trend as that for the full-length ligands, that is mutation of valine to tyrosine enhances and valine to alanine decreases the capacity of the GPR15L fragment to activate ERK1/2 (Fig. 7C). In addition, we compared the rate of receptor endocytosis induced by the C-terminal 18-mer peptides to further confirm the relative efficacy of the C-terminal residues in the receptor signaling. Based on the reported β-arrestin recruitment by GPR15L (Ocón et al., 2017), the ligand-induced endocytosis of GPR15 will most likely represent the outcome of the β-arrestin recruitment, although other pathways may also be involved in the GPCR endocytosis (Bhatnagar et al., 2001). Stimulation with V57Y and V57A peptides induced significantly higher and lower endocytosis rates than WT, respectively, at all the concentrations tested (Fig. 7D). Overall, our results together demonstrate that the C-terminal amino acid of GPR15L critically contributes to the receptor binding through a mechanism that

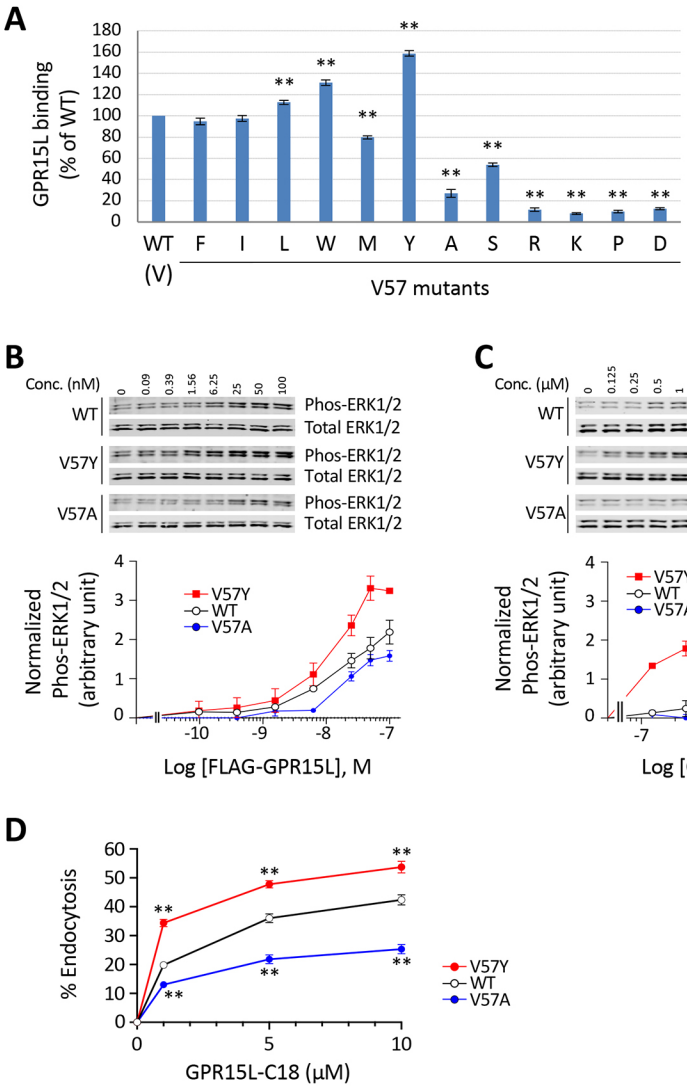

Fig. 7. Hydrophobicity of the extreme C-terminal residue of GPR15L is important for receptor binding and activation. (A) HEK293 cells transfected with GPR15 were subjected to FLAG–GPR15L binding using the culture supernatants shown in Fig. S4A. (B) Effects of C-terminal mutations of GPR15L on the ERK1/2 activation. HEK293 cells transfected with untagged GPR15 were stimulated with the indicated amounts of purified WT, V57Y and V57A FLAG–GPR15L (see Fig. S4B for purity analysis) and lysates were analyzed for the ERK1/2 activation. Upper panels show representative blot images from three experiments. The phospho-ERK1/2 signals from GPR15L-treated cells were subtracted with those of no-ligand controls and then normalized with respect to the signals of total ERK1/2 (bottom panel). (C) Effects of C-terminal mutations of 18-mer GPR15L peptides on the ERK1/2 activation. HEK293 cells stably expressing untagged GPR15 receptor were stimulated with C-18 peptides and analyzed for the ERK1/2 activation. Upper panels show representative blot images from three experiments; lower panels show the quantification. (D) Effects of C-terminal mutations of 18-mer GPR15L peptides on the receptor endocytosis. HEK293 cells stably expressing untagged GPR15 were incubated with C-18 peptides for 60 min at 37°C and stained with BV421–GPR15 Ab. Cells treated with ligands and kept at 4°C served for controls. The endocytosis rate (%) was determined by dividing the difference of fluorescence between 4°C control and post-37°C incubation by the 4°C control value. Quantitative results are mean±s.e.m. (n=3). $^{**}P \leq 0.01$ from WT (Student's t-test).

Journal of Cell Science (2021) 134, jcs247833. doi:10.1242/jcs.247833

plausibly involves its hydrophobic nature, and that this impacts the receptor signaling.

DISCUSSION

GPR15L (C10orf99) has been reported to have a multitude of functions in addition to being the chemoattractant ligand activity for GPR15. It exhibits antimicrobial activity, which inhibits the growth of bacteria, fungi and viruses (Yang et al., 2015). GPR15L also promotes cutaneous wound healing (Li et al., 2015) and can prospectively contribute to the development of psoriasis by promoting the keratinocyte proliferation (Chen et al., 2018). GPR15L has also been reported to bind to SUSD2 on the colon cancer cells and inhibit their growth, although this effect might depend on the C-terminal tagging of GPR15L (Pan et al., 2014; Yang et al., 2015). In addition, the GPR15 receptor has been recently found to interact with thrombomodulin and mediate cytoprotective and pro-angiogenic activities in endothelial cells (Wang et al., 2018). These apparently GPR15 receptor-independent activities of GPR15L, as well as GPR15L-independent activity of GPR15 receptor, raise the importance of accurately defining the biochemical nature of the GPR15–GPR15L interaction, as such information might be essential for interventions specifically targeting this signaling axis.

In this study, we utilized a FLAG epitope to tag the GPR15L protein for detection and purification purposes. However epitope tags, such as FLAG, that contain charged residues could affect the binding properties of GPR15L. To address this concern, we also attempted the binding assays using the untagged synthetic GPR15L peptide and commercial anti-GPR15L Abs that we found are able to immunoprecipitate GPR15L (data not shown). Notwithstanding our best efforts, we were unable to detect the receptor-bound form of the ligand, probably because of the steric hindrance of the Ab-binding epitope. However, it is important to remark that the functional assays in Figs 4 and 7 using the untagged GPR15L peptides all showed results consistent with the binding profiles of the FLAG-tagged ligands, suggesting that the FLAG tagging of GPR15L does not affect the nature of its receptor binding to GPR15L, at least with regard to the sensitivity to the receptor modifications as well as modification to the ligand C-terminal residue.

N-terminal tyrosine sulfation has been shown to enhance affinity and selectivity of chemokine binding in numerous chemokine receptors (Farzan et al., 2002; Fong et al., 2002; Scurci et al., 2021; Tan et al., 2013; Zhu et al., 2011). This body of evidence indicates the importance of understanding chemokine receptor sulfation for an insightful understanding of both chemokine cell biology and for the development of drugs targeting chemokine receptors. Structural studies have asserted that the negatively charged sulfotyrosine binds into an electropositive groove on the chemokine surface (Millard et al., 2014). Our study demonstrated that the GPR15 receptor is sulfated on at least one of the N-terminal tyrosine residues and that this sulfation promotes binding of GPR15L both in a transfected HEK293 cell and the T cell line HuT78 expressing endogenous GPR15. Since GPR15L is rich in basic residues, as are the other classic chemokines, sulfotyrosines of GPR15 likely increase the binding affinity to ligand primarily through electrostatic interaction. However, our ERK1/2 assay raised an interesting possibility of sulfated tyrosine residues also contributing to the ligand binding through an electrostatic-independent mechanism. The ERK1/2 activation by C-terminal 11-mer peptide, which contains no charged residue, was also attenuated by the Y/F mutation, implying the interaction of tyrosine residues with non-charged residues in the ligand C-terminus. This notion is supported by the nuclear magnetic resonance structure of the CXCR4–CXCL12 complex, which reveals that sulfated tyrosine of CXCR4 forms hydrophobic interactions with two valine residues as well as arginine residue in the binding pocket of CXCL12 (Veldkamp et al., 2008). It is, thus, possible that the N-terminal tyrosine residues promote receptor binding of the C-terminal domain of GPR15L through interaction with the hydrophobic residues. Therefore, extensive structural studies are warranted to further define the role of N-terminal sulfotyrosines in the receptor binding of GPR15L C-terminal domain.

Compared with tyrosine sulfation, the existing body of knowledge regarding the role of receptor O-glycosylation in chemokine binding and receptor signaling is fairly limited. In CCR5 and CCR8, O-glycosylation on the N-terminal threonine and serine residues has been shown to positively contribute to the binding of their cognate ligands (Bannert et al., 2001; Gutiérrez et al., 2004). We adopted three different approaches to determine the impact of receptor O-glycosylation on the binding of GPR15L. First, the alanine mutation of threonine and serine residues (TS/AA), which abolished O-glycosylation, resulted in the increased binding of GPR15L. Second, conditional induction of O-glycosylation on GPR15 receptor in the ldlD mutant CHO cell led to the decreased binding of GPR15L. Third, sialic acid removal by neuraminidase resulted in the increased ligand binding to WT but not the TS/AA mutant receptor. The presence of α2,3-linked sialic acids on GPR15 and their inhibitory role in ligand binding were also observed in the human T cell line HuT 78. These results collectively corroborate the notion that the receptor O-glycosylation negatively regulates the GPR15L binding and that the α2,3-linked sialic acids that cap O-glycans are at least partly responsible for this inhibition. In essence, the enhanced ERK1/2 signaling in the O-glycosylation-deficient GPR15 mutant (TS/AA) demonstrates the functional relevance of O-glycan-mediated regulation of GPR15L binding. Thus, our findings reveal that GPR15 represents a unique chemoattractant receptor in which the N-terminal O-glycosylation and tyrosine sulfation play contrasting roles in the ligand binding, which is distinct from their reportedly cooperative roles in the ligand binding of CCR5 and CCR8 (Bannert et al., 2001; Gutiérrez et al., 2004). Our working model of the PTM-regulated GPR15–GPR15L interaction is schematically depicted in Fig. 8.

How do the O-glycans inhibit GPR15L binding? Based on the fact that the threonine and serine residues are adjacent to the tyrosine residues within the N-terminus, O-glycans may prevent ligand from accessing the sulfated tyrosine. However, the enhancement of ligand binding by the neuraminidase treatment even in the absence of tyrosine residues (Y/F mutant) suggests that the O-glycans also inhibit the ligand access to the receptor regions independently of tyrosine residues, such as ECL and TM segments (Fig. 8). Since the ERK1/2 activation by the C-13 and C-11 fragment ligands containing no acidic residue was also increased by TS/AA mutation, the O-glycan/sialic acids on GPR15 may sterically block the binding of GPR15L, as has been reported for CCR7 and its ligands (Hauser et al., 2016), rather than by the charge repulsion mechanism.

PTMs such as tyrosine sulfation and glycosylation/sialylation represent a highly regulated enzymatic processes. Yyrosine sulfation of CXCR4 is upregulated by the Epstein–Barr virus-encoded protein LMP1, which enhances the expression of the tyrosylprotein sulfotransferase TPST-1, which in turn enhances chemotaxis of CXCR4-expressing cells (Xu et al., 2013). Such alteration of TPST-1 expression will conceivably influence the ligand-binding affinity of other GPCRs, including GPR15. Moreover, the expression of sialyltransferases ST3Gal1 and ST6Gal1 is known to be decreased by the activation of T cells, leading to the reduction of α2,3- and α2,6-linked sialic acids on the cell surface (Villanueva-Cabello et al.,

Journal of Cell Science (2021) 134, jcs247833. doi:10.1242/jcs.247833

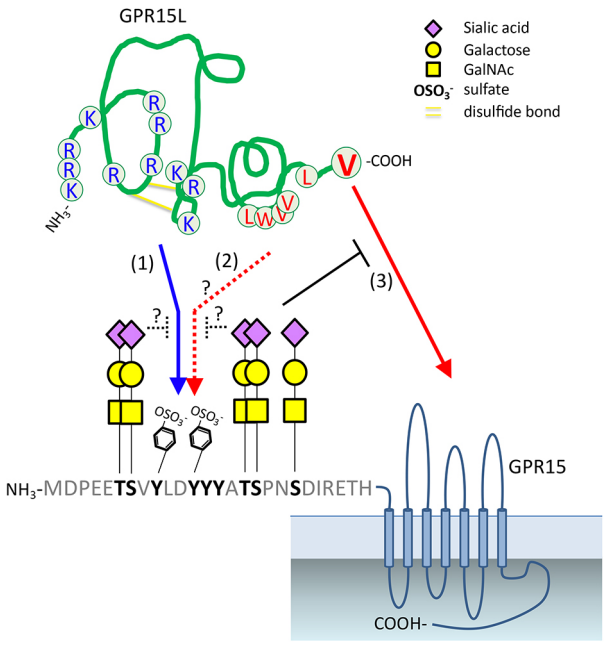

Fig. 8. Schematic working model of the differential regulation of GPR15L binding by the tyrosine sulfation and O-glycosylation of GPR15 receptor. The GPR15–GPR15L interaction and its regulation involving the sulfated tyrosine and O-glycosylated threonine and serine residues are depicted. The GPR15L protein was manually drawn with reference to the predicted model published previously (Suply et al., 2017). The exact positions of the tyrosine and threonine and serine residues that are actually sulfated or O-glycosylated were not mapped in this study. (1) The sulfated tyrosine residues in the GPR15 N-terminus promote GPR15L binding most likely through the electrostatic interaction with the basic residues (highlighted in blue) of the ligand. (2) The tyrosine residues potentially also contribute to the ligand binding by forming a hydrophobic interaction with the C-terminal hydrophobic residues (highlighted in red) of the ligand. (3) The hydrophobic residue at the extreme C-terminus (V57) of GPR15L plays a crucial role in the binding to GPR15 presumably by interacting with the ECL and/or TM segments of the receptor. This, and possibly other interactions involving upstream regions of GPR15L, are inhibited by the sialylated O-glycans on the N-terminal threonine and serine residues of GPR15.

2015). T cell activation also induces the increased expression of a distinct form of sialidase (Neu1), which reduces the cell surface sialic acid level (Nan et al., 2007). Furthermore, mature monocyte-derived dendritic cells secrete glycosidases that desialylate CCR7 on T cells, boosting CCR7-mediated migration toward its chemokine ligand (Hauser et al., 2016). These observations underpin the conception that the strength of the GPR15–GPR15L interaction is dynamically regulated in both physiological and pathological conditions through alterations of tyrosine sulfation and O-glycosylation/sialylation on the GPR15 receptor.

The members of chemokine family share conserved secondary and tertiary structure; a flexible N-terminus and N-terminal loop followed by a three-stranded β-sheet and a single α-helix on the C-terminus (Lubman and Fremont, 2016). However, GPR15L has been reported to have no predictable preference for the formation of β-strands and helices (Suply et al., 2017). A widely accepted two-step/two-site model entails the recognition of chemokine core domain (N-loop and β3 regions, site one) by the receptor N-terminal tail followed by the activation of receptor through docking of chemokine flexible N-terminus (site two) to the ECL and TM segments (Rajagopalan and Rajarathnam, 2006). Consistent with this model, the truncation or mutation of chemokine N-terminus has often been found to alter its receptor binding affinity (Clark-Lewis et al., 1991) as well as agonistic or antagonistic activity (Loetscher and Clark-Lewis, 2001). In the case of GPR15L, however, the truncation of the N-terminal residues up to 10 aa does not affect its ability to induce Ca^{2+} signaling downstream of GPR15 (Suply et al., 2017), suggesting a relatively smaller contribution for the N-terminal tail. Instead, previous studies (Foster et al., 2019; Ocón et al., 2017; Suply et al., 2017) and our ERK1/2 assays demonstrate a capacity of the C-terminal domain of GPR15L to activate GPR15 signaling. Our truncation study revealed that the extreme C-terminal residue (V57) of GPR15L is critically required for its binding to the receptor. The amino acid extension of ligand C-terminus by even one residue considerably reduced its binding to the receptor (data not shown), further supporting the importance of C-terminal integrity of GPR15L. Moreover, the absence of FLAG–GPR15L binding to a chimeric CXCR4 receptor with the GPR15 N-terminal tail indicates a strict requirement of ECL and/or TM domains of GPR15 receptor for the GPR15L binding. Collectively, these results suggest that the interaction of C-terminal V57, presumably with the ECL and/or TM segments of the receptor, leads to the ligand binding to and activation of GPR15 (Fig. 8). The strict requirement of C-terminal residues for receptor binding is uncommon for chemokine family proteins. One rather well-characterized example is C5a, a chemoattractant protein fragment released from proteolytic cleavage of complement component C5, where the C-terminal cationic domain is required for optimal binding to and activation of C5a receptor (Reis et al., 2012). Our mutagenesis study of the C-terminal V57 indicated that the hydrophobic residues are favored at this position for receptor binding. Interestingly, the tyrosine residue, which is customarily not regarded as the most hydrophobic amino acid, was significantly more effective than valine in conferring receptor binding and ERK1/2 activation. This implies additional attributes of the C-terminal residue contribute to the receptor interaction. Our findings suggest that engineering of the C-terminal tail can potentially develop GPR15 ligands with modified affinity and activity.

MATERIALS AND METHODS

Plasmids

The human GPR15 gene was cloned into the pCDNA3.1(+) vector (Invitrogen) and pCMVmyc vector (Okamoto and Shikano, 2011) to generate untagged and N-terminally Myc-tagged GPR15 plasmid, respectively. The pCDNA-C10orf99 plasmid (Genscript) was used as a PCR template to generate pCDNA-FLAG-GPR15L, which carries a FLAG (DYKDDDDK) epitope right after the 24 aa signal sequence. Site-directed mutagenesis was performed by the overlap extension PCR. Chimeric CXCR4 was generated by replacing the N-terminal extracellular domain of human CXCR4 (aa 1–38) with that of human GPR15 (aa 1–33).

Reagents

The following reagents were used in this study: sodium chlorate, neuraminidase (*Arthrobacter ureafaciens* and *Vibrio cholerae*), puromycin and anti-FLAG affinity resin from Sigma-Aldrich; DYKDDDDK peptide and 18-mer (aa 40–57), 13-mer (aa 45–57), and 11-mer (aa 47–57) peptides encoding the C-terminus of GPR15L from Genscript and Biomatik; and full-length synthetic GPR15L peptide (aa 1–57) with disulfide bridges at aa 16/39 and aa 17/36 from Phoenix Pharmaceuticals.

Antibodies and lectins

The following Abs were used: mouse anti-GPR15 (#MAB3654, 2 µg/ml) from R&D Systems, rabbit anti-GPR15 C-terminus (#PA5-33643, 1:1000), rabbit anti-C10orf99 (#PA5-62266, termed anti-GPR15L Ab in this study, 1:1000) from Thermo Fisher Scientific, mouse anti-Myc (#05-724, 1:1000) and Alexa Fluor (AF) 488-mouse anti-Myc (#16-224, 1:500) from EMD Millipore, Brilliant Violet 421 (BV421)-mouse-anti-GPR15 (#373007, 1:100), BV421-mouse IgG2a (#400259, 1:100), rat anti-DYKDDDDK

Journal of Cell Science (2021) 134, jcs247833. doi:10.1242/jcs.247833

(#637301, 1:500), phycoerythrin (PE)-rat anti-DYKDDDDK (#637309, 1:400–1:1000), purified rabbit polyclonal control Ab (#910805, 1:1000), and PE-streptavidin (#405203, 1:400) from BioLegend, rabbit phospho-p44/42 MAPK (#9101, 1:1000) and mouse p44/42 MAPK (#9107, 1:1000) from Cell Signaling Technology, AF488-goat anti-mouse IgG H+L (#A11001, 1:1000) PE-goat anti-mouse IgG H+L (#PA1-84395, 1:1000) from Invitrogen, horseradish peroxidase (HRP)-goat anti-rabbit-IgG (#111-036-003, 1:2000) from Jackson ImmunoResearch Laboratory, HRP-horse anti-mouse-IgG (#PI-2000, 1:2000), Biotin-*Maackia amurensis* lectin II (MALII) (#B-1265, 0.5–1 µg/ml), and Biotin-*Sambucus nigra* lectin (SNA) (B-1305, 0.1 µg/ml) from Vector Laboratory, 680RD-goat anti-rabbit IgG (#926-68073, 1:15,000), 680RD-goat anti-rat IgG (#926-68076, 1:15,000), and 800CW-goat anti-mouse IgG (#926-32210, 1:15,000) from LI-COR Biosciences, HRP-streptavidin (#SA202, 1:2000) from Sigma-Aldrich.

Cell culture and transfection

HEK293 and HEK293T cells (both ATCC) were maintained in 50% DMEM/50% Ham's F-12 and DMEM, respectively, both containing 10% FBS, 2 mM L-glutamine, 100 U/ml penicillin, and 100 µg/ml streptomycin. Chinese hamster ovary (CHO) ldlD cells (provided by Dr Monty Krieger, Department of Biology, Massachusetts Institute of Technology, USA) were maintained in Ham's F-12 with 5% FBS, 2 mM L-glutamine, 100 U/ml penicillin, and 100 µg/ml streptomycin. The HuT 78T cell lymphoma line (ATCC) was maintained in RPMI 1640 containing 20% FBS, 2 mM L-glutamine, 100 U/ml penicillin and 100 µg/ml streptomycin. All cell culture media were purchased from Corning, unless otherwise stated. According to the manufacturer's instructions, transient transfection of plasmids was performed using Mirus TransIT-LT1 (Mirus Bio). Both GPR15-overexpressing HuT 78 cells and stable GPR15-expressing HEK293 cells were generated by retroviral transfection of GPR15 using the culture supernatants of Phoenix ampho packaging cells (ATCC) transfected with pBABEpuro-GPR15, and cell populations resistant to puromycin were selected.

SDS-PAGE and western blotting

Cell lysates were made by using lysis buffer (0.5% Igepal, 25 mM Tris-HCl pH 7.150 mM NaCl, 5) containing a protease inhibitor cocktail. The protein samples resolved on Tris-HCl polyacrylamide gels were transferred to nitrocellulose membranes and blocked with skim milk or blocking buffer (LI-COR Biosciences). The membranes were first incubated with primary Abs overnight at 4°C and then with the appropriate HRP-conjugated or near-infrared fluorescent dye-conjugated secondary Abs. Blot signals were quantitatively analyzed by Azure c300 (Azure Biosystems) for chemiluminescence or Odyssey CLx (LI-COR Biosciences) for near-infrared fluorescence.

Flow cytometry

Fluorescence signal of the Ab-stained cells was measured using Cell Lab Quanta SC or CytoFLEX S (Beckman Coulter) and analyzed using FlowJo software (Tree Star).

[^{35}S]sulfate metabolic labeling

HEK293 cells were transfected in 10 cm dishes with vector or Myc–GPR15 constructs, and 4 h later culture medium was replaced with 7 ml of sulfate-free Joklik-modified minimum essential medium Eagle (JMEM) (Sigma-Aldrich) supplemented with 1 mM $CaCl_2$, 10% dialyzed FBS (Sigma-Aldrich) and 10 mM sodium chlorate or vehicle. Subsequent to that, 250 µCi sodium [^{35}S]sulfate (Perkin Elmer) was added and cells were cultured overnight. After washing, the labeled cells were lysed with 0.5% Igepal lysis buffer, and the GPR15 proteins were immunoprecipitated with 5 µg of anti-Myc Ab. The eluants were analyzed by SDS-PAGE followed by autoradiography of the transfer membranes by Storm Molecular Imager (Molecular Dynamics). Eventually, the same membranes were probed for Myc signal by western blotting.

Recombinant FLAG–GPR15L protein

HEK293T cells were transfected with pCDNA-FLAG-GPR15L and the culture medium was replaced with a fresh medium at 48 h after transfection. The culture supernatant was collected 24 h later and incubated overnight with anti-FLAG Ab-conjugated resin at 4°C. After an extensive wash with 0.1% Triton X-100-containing PBS (PBST, pH 7.4), the resin was incubated with PBST containing 100 µg/ml FLAG peptide to elute FLAG–GPR15L protein. Triton X-100 remaining in the eluant was removed with a HiPPR Detergent Removal Spin Column kit (Thermo Fischer Scientific). The concentration of FLAG–GPR15L in the eluant or culture supernatant was determined by western blotting with anti-GPR15L Ab using known amounts of synthetic GPR15L peptide as a standard (Fig. S1A).

FLAG–GPR15L binding assay

HEK293 cells transfected with Myc–GPR15 or untagged GPR15 plasmid were collected by gentle pipetting and then incubated with purified FLAG–GPR15 or culture supernatants containing FLAG–GPR15 for 45 min at 4°C. After a wash with Hanks' balanced salt solution supplemented with 1% BSA (staining buffer), cells were further incubated with PE-anti-FLAG Ab for 20 min at 4°C. In the experiments where cells were transfected with different Myc–GPR15 constructs or treated with reagents and compared for FLAG–GPR15L binding, the cells were stained with both AF488-anti-Myc and PE-anti-FLAG Abs at the same time after FLAG–GPR15L binding. The stained cells were then washed with staining buffer and stored in 1% paraformaldehyde-PBS solution at 4°C until FCM analysis. For GPR15L binding to CHO ldlD, the cells were cultured in Ham's F-12 containing 3% dialyzed FBS and ITS (insulin-transferrin-selenium) one day prior to the transfection. At 3 h after the transfection with Myc–GPR15, vehicle or N-acetylgalactosamine (GalNAc) and galactose were added to the culture at 200 µM and 20 µM, respectively. The next day, the cells were harvested by quick trypsinization and then cultured again in the same medium containing 2 mM EDTA for 2 h at 37°C to allow recovery of surface GPR15 expression. The cells were then collected with gentle pipetting and subjected to surface Myc–GPR15 staining and FLAG–GPR15L binding as described for HEK293 cells. For GPR15L binding to HuT 78, the cells were treated with neuraminidase or sodium chlorate and subjected to surface GPR15 staining using BV421-anti-GPR15 Ab as well as to FLAG-GPR15L binding.

Neuraminidase treatment of cells

HEK293 cells transfected with Myc–GPR15 or GPR15-overexpressing HuT 78 cells were incubated for 1 h at 37°C in 150 µl of DMEM containing 0.1% sodium azide and 1% FBS (HEK293) or for 30 min at 37°C in 150 µl of RPMI1640 containing 0.1% sodium azide and 1% FBS (HuT 78) and neuraminidase from either *A. ureafaciens* (400 mU/ml) or *V. cholerae* (20 mU/ml). The cells were washed and subjected to FLAG–GPR15L binding, lectin binding or immunoprecipitation of GPR15.

Lectin-binding assays

For assessing the effect of neuraminidase on cell surface sialic acids, GPR15-transfected HEK293 cells or HuT 78 cells treated or not with neuraminidase were incubated for 30 min at 4°C with 1 µg/ml of Biotin-MALII or 0.1 µg/ml of Biotin-SNA. The cells were washed and further stained with PE–streptavidin for 20 min and analyzed by FCM. For testing sialylation of GPR15 in HuT 78 cells, the GPR15 proteins were immunoprecipitated with anti-GPR15 C-terminus Ab from cells treated or not with neuraminidase and the eluants were immunoblotted with Biotin-MALII at 0.5 µg/ml for 1 h at room temperature, followed by incubation with HRP–streptavidin for 20 min at room temperature. The signals were detected by chemiluminescence.

ERK1/2 activation assay

ERK1/2 activation assays were performed in either 24-well or 96-well format. For the former, HEK293 cells plated in poly-lysine-coated 24-well plates were transfected with Myc-tagged GPR15. The following day, the cells were stimulated with either purified FLAG–GPR15, FLAG–GPR15L-containing culture supernatant, full-length synthetic GPR15L (aa 1–57), or C-terminal fragment peptides for 4 min at 37°C, then lysed and the centrifuged supernatants (13,000 ***g*** for 5 min) were subjected to simultaneous blotting for phosphorylated and total ERK1/2 proteins. For the 96-well format, cells

transfected in 6-well plates with Myc-tagged or untagged GPR15 were collected after 24 h and re-plated in 96-well plates. For the indicated experiments, a HEK293 cell line stably expressing GPR15 was used. After serum-starved for 1 h at 37°C, cells were stimulated with GPR15L for 1 min 45 s at 37°C. After centrifugation of plates at 2000 ***g*** for 1 min at 4°C and removal of the supernatants, the cells were lysed and the centrifuge supernatants were subjected to ERK1/2 blot. The band intensities were measured by near-infrared fluorescence imaging. The phospho-ERK1/2 signals were normalized with respect to the signals of total ERK1/2.

Endocytosis assay

HEK293 cells stably expressing untagged GPR15 were incubated with the indicated concentrations of C-terminal 18-mer GPR15L peptides for 60 min at 37°C to allow for receptor internalization. After cells were chilled on ice, the surface expression level of the GPR15 receptor was measured by staining with BV421-anti-GPR15 Ab followed by FCM. Cells treated with each concentration of ligands and incubated at 4°C were also stained for controls. We have confirmed that the prior binding of the ligand does not interfere with the GPR15 Ab binding to the receptor (data not shown). The endocytosis rate (%) was determined by dividing the difference in fluorescence between 4°C control and post-37°C incubation by the 4°C control value.

Statistical analysis

Data are shown as means±s.e.m. of triplicate samples from three independent experiments. The statistical significance was assessed with the two-tailed Student's *t*-test between a pair of datasets and values of $P<0.05$ were considered significant.

Competing interests

The authors declare no competing or financial interests.

Author contributions

Conceptualization: S.S., Y.O.; Methodology: S.S., Y.O.; Validation: S.S.; Formal analysis: S.S., Y.O.; Investigation: S.S., Y.O.; Data curation: S.S., Y.O.; Writing - original draft: S.S., Y.O.; Writing - review & editing: S.S., Y.O.; Supervision: S.S.; Project administration: S.S.; Funding acquisition: S.S.

Funding

This study was supported by grants from National Institutes of Health grants NIGMS (R01GM099974) and NIAID (R21AI142060) for S.S. Deposited in PMC for release after 12 months.

References

Bannert, N., Craig, S., Farzan, M., Sogah, D., Santo, N. V., Choe, H. and Sodroski, J. (2001). Sialylated O-glycans and sulfated tyrosines in the NH2-terminal domain of CC chemokine receptor 5 contribute to high affinity binding of chemokines. *J. Exp. Med.* **194**, 1661-1673. doi:10.1084/jem.194.11.1661

Bauer, M., Hackermuller, J., Schor, J., Schreiber, S., Fink, B., Pierzchalski, A. and Herberth, G. (2018). Specific induction of the unique GPR15 expression in heterogeneous blood lymphocytes by tobacco smoking. *Biomarkers* **24**, 217-224. doi:10.1080/1354750X.2018.1539769

Bhatnagar, A., Willins, D. L., Gray, J. A., Woods, J., Benovic, J. L. and Roth, B. L. (2001). The dynamin-dependent, arrestin-independent internalization of 5-hydroxytryptamine 2A (5-HT2A) serotonin receptors reveals differential sorting of arrestins and 5-HT2A receptors during endocytosis. *J. Biol. Chem.* **16**, 8269-8277. doi:10.1074/jbc.M006968200

Bundgaard, J. R., Vuust, J. and Rehfeld, J. F. (1997). New consensus features for tyrosine O-sulfation determined by mutational analysis. *J. Biol. Chem.* **272**, 21700-21705. doi:10.1074/jbc.272.35.21700

Byrne, B., Donohoe, G. G. and O'Kennedy, R. (2007). Sialic acids: carbohydrate moieties that influence the biological and physical properties of biopharmaceutical proteins and living cells. *Drug Discov. Today* **12**, 319-326. doi:10.1016/j.drudis.2007.02.010

Chen, C., Wu, N., Duan, Q., Yang, H., Wang, X., Yang, P., Zhang, M., Liu, J., Liu, Z., Shao, Y. et al. (2018). C10orf99 contributes to the development of psoriasis by promoting the proliferation of keratinocytes. *Sci. Rep.* **8**, 8590. doi:10.1038/s41598-018-26996-z

Clark-Lewis, I., Schumacher, C., Baggiolini, M. and Moser, B. (1991). Structure-activity relationships of interleukin-8 determined using chemically synthesized analogs. Critical role of NH2-terminal residues and evidence for uncoupling of neutrophil chemotaxis, exocytosis, and receptor binding activities. *J. Biol. Chem.* **266**, 23128-23134. doi:10.1016/S0021-9258(18)54472-0

Deng, H. K., Unutmaz, D., KewalRamani, V. N. and Littman, D. R. (1997). Expression cloning of new receptors used by simian and human immunodeficiency viruses. *Nature* **388**, 296-300. doi:10.1038/40894

Farzan, M., Mirzabekov, T., Kolchinsky, P., Wyatt, R., Cayabyab, M., Gerard, N. P., Gerard, C., Sodroski, J. and Choe, H. (1999). Tyrosine sulfation of the amino terminus of CCR5 facilitates HIV-1 entry. *Cell* **96**, 667-676. doi:10.1016/S0092-8674(00)80577-2

Farzan, M., Babcock, G. J., Vasilieva, N., Wright, P. L., Kiprilov, E., Mirzabekov, T. and Choe, H. (2002). The role of post-translational modifications of the CXCR4 amino terminus in stromal-derived factor 1 alpha association and HIV-1 entry. *J. Biol. Chem.* **277**, 29484-29489. doi:10.1074/jbc.M203361200

Fischer, A., Zundler, S., Atreya, R., Rath, T., Voskens, C., Hirschmann, S., Lopez-Posadas, R., Watson, A., Becker, C., Schuler, G. et al. (2016). Differential effects of alpha4beta7 and GPR15 on homing of effector and regulatory T cells from patients with UC to the inflamed gut in vivo. *Gut* **65**, 1642-1664. doi:10.1136/gutjnl-2015-310022

Fong, A. M., Alam, S. M., Imai, T., Haribabu, B. and Patel, D. D. (2002). CX3CR1 tyrosine sulfation enhances fractalkine-induced cell adhesion. *J. Biol. Chem.* **277**, 19418-19423. doi:10.1074/jbc.M201396200

Foster, S. R., Hauser, A. S., Vedel, L., Strachan, R. T., Huang, X. P., Gavin, A. C., Shah, S. D., Nayak, A. P., Haugaard-Kedstrom, L. M., Penn, R. B. et al. (2019). Discovery of Human Signaling Systems: Pairing Peptides to G Protein-Coupled Receptors. *Cell* **179**, 895-908.e21.

Gahmberg, C. G. and Andersson, L. C. (1982). Role of sialic acid in the mobility of membrane proteins containing O-linked oligosaccharides on polyacrylamide gel electrophoresis in sodium dodecyl sulfate. *Eur. J. Biochem.* **122**, 581-586. doi:10.1111/j.1432-1033.1982.tb06478.x

Gao, J., Choe, H., Bota, D., Wright, P. L., Gerard, C. and Gerard, N. P. (2003). Sulfation of tyrosine 174 in the human C3a receptor is essential for binding of C3a anaphylatoxin. *J. Biol. Chem.* **278**, 37902-37908. doi:10.1074/jbc.M306061200

Goh, J. B. and Ng, S. K. (2018). Impact of host cell line choice on glycan profile. *Crit. Rev. Biotechnol.* **38**, 851-867. doi:10.1080/07388551.2017.1416577

Gutiérrez, J., Kremer, L., Zaballos, A., Goya, I., Martínez, A. C. and Márquez, G. (2004). Analysis of post-translational CCR8 modifications and their influence on receptor activity. *J. Biol. Chem.* **279**, 14726-14733. doi:10.1074/jbc.M309689200

Hauser, M. A., Kindinger, I., Laufer, J. M., Späte, A.-K., Bucher, D., Vanes, S. L., Krueger, W. A., Wittmann, V. and Legler, D. F. (2016). Distinct CCR7 glycosylation pattern shapes receptor signaling and endocytosis to modulate chemotactic responses. *J. Leukoc. Biol.* **99**, 993-1007. doi:10.1189/jlb.2VMA0915-432RR

Kim, S. V., Xiang, W. V., Kwak, C., Yang, Y., Lin, X. W., Ota, M., Sarpel, U., Rifkin, D. B., Xu, R. and Littman, D. R. (2013). GPR15-mediated homing controls immune homeostasis in the large intestine mucosa. *Science* **340**, 1456-1459. doi:10.1126/science.1237013

Kingsley, D. M. and Krieger, M. (1984). Receptor-mediated endocytosis of low density lipoprotein: somatic cell mutants define multiple genes required for expression of surface-receptor activity. *Proc. Natl. Acad. Sci. USA* **81**, 5454-5458. doi:10.1073/pnas.81.17.5454

Kleist, A. B., Getschman, A. E., Ziarek, J. J., Nevins, A. M., Gauthier, P.-A., Chevigne, A., Szpakowska, M. and Volkman, B. F. (2016). New paradigms in chemokine receptor signal transduction: Moving beyond the two-site model. *Biochem. Pharmacol.* **114**, 53-68. doi:10.1016/j.bcp.2016.04.007

Kõks, S. and Kõks, G. (2017). Activation of GPR15 and its involvement in the biological effects of smoking. *Exp. Biol. Med. (Maywood)* **242**, 1207-1212. doi:10.1177/1535370217703977

Lahl, K., Sweere, J., Pan, J. and Butcher, E. (2014). Orphan chemoattractant receptor GPR15 mediates dendritic epidermal T-cell recruitment to the skin. *Eur. J. Immunol.* **44**, 2577-2581. doi:10.1002/eji.201444628

Li, X., Fan, R., Tong, A., Yang, M., Deng, J., Zhou, L., Zhang, X. and Guo, G. (2015). In situ gel-forming AP-57 peptide delivery system for cutaneous wound healing. *Int. J. Pharm.* **495**, 560-571. doi:10.1016/j.ijpharm.2015.09.005

Loetscher, P. and Clark-Lewis, I. (2001). Agonistic and antagonistic activities of chemokines. *J. Leukoc. Biol.* **69**, 881-884.

Lubman, O. Y. and Fremont, D. H. (2016). Parallel evolution of chemokine binding by structurally related herpesvirus decoy receptors. *Structure* **24**, 57-69. doi:10.1016/j.str.2015.10.018

Millard, C. J., Ludeman, J. P., Canals, M., Bridgford, J. L., Hinds, M. G., Clayton, D. J., Christopoulos, A., Payne, R. J. and Stone, M. J. (2014). Structural basis of receptor sulfotyrosine recognition by a CC chemokine: the N-terminal region of CCR3 bound to CCL11/eotaxin-1. *Structure* **22**, 1571-1581. doi:10.1016/j.str.2014.08.023

Mizoue, L. S., Sullivan, S. K., King, D. S., Kledal, T. N., Schwartz, T. W., Bacon, K. B. and Handel, T. M. (2001). Molecular determinants of receptor binding and signaling by the CX3C chemokine fractalkine. *J. Biol. Chem.* **276**, 33906-33914. doi:10.1074/jbc.M101348200

Nan, X., Carubelli, I. and Stamatos, N. M. (2007). Sialidase expression in activated human T lymphocytes influences production of IFN-gamma. *J. Leukoc. Biol.* **81**, 284-296. doi:10.1189/jlb.1105692

Nguyen, L. P., Pan, J., Dinh, T. T., Hadeiba, H., O'Hara, E., III, Ebtikar, A., Hertweck, A., Gokmen, M. R., Lord, G. M., Jenner, R. G. et al. (2015). Role and

species-specific expression of colon T cell homing receptor GPR15 in colitis. *Nat. Immunol.* **16**, 207-213. doi:10.1038/ni.3079

Nørskov-Lauritsen, L., Jørgensen, S. and Bräuner-Osborne, H. (2015). N-glycosylation and disulfide bonding affects GPRC6A receptor expression, function, and dimerization. *FEBS Lett.* **589**, 588-597. doi:10.1016/j.febslet.2015.01.019

Ocón, B., Pan, J., Dinh, T. T., Chen, W., Ballet, R., Bscheider, M., Habtezion, A., Tu, H., Zabel, B. A. and Butcher, E. C. (2017). A mucosal and cutaneous chemokine ligand for the lymphocyte chemoattractant receptor GPR15. *Front Immunol* **8**, 1111. doi:10.3389/fimmu.2017.01111

Okamoto, Y. and Shikano, S. (2011). Phosphorylation-dependent C-terminal binding of 14-3-3 proteins promotes cell surface expression of HIV co-receptor GPR15. *J. Biol. Chem.* **286**, 7171-7181. doi:10.1074/jbc.M110.199695

Okamoto, Y. and Shikano, S. (2017). Differential phosphorylation signals control endocytosis of GPR15. *Mol. Biol. Cell* **28**, 2267-2281. doi:10.1091/mbc.e16-09-0627

Pan, W., Cheng, Y., Zhang, H., Liu, B., Mo, X., Li, T., Li, L., Cheng, X., Zhang, L., Ji, J. et al. (2014). CSBF/C10orf99, a novel potential cytokine, inhibits colon cancer cell growth through inducing G1 arrest. *Sci. Rep.* **4**, 6812. doi:10.1038/srep06812

Petäjä-Repo, U. E., Hogue, M., Laperrière, A., Walker, P. and Bouvier, M. (2000). Export from the endoplasmic reticulum represents the limiting step in the maturation and cell surface expression of the human delta opioid receptor. *J. Biol. Chem.* **275**, 13727-13736. doi:10.1074/jbc.275.18.13727

Rajagopalan, L. and Rajarathnam, K. (2006). Structural basis of chemokine receptor function–a model for binding affinity and ligand selectivity. *Biosci. Rep.* **26**, 325-339. doi:10.1007/s10540-006-9025-9

Reis, E. S., Chen, H., Sfyroera, G., Monk, P. N., Kohl, J., Ricklin, D. and Lambris, J. D. (2012). C5a receptor-dependent cell activation by physiological concentrations of desarginated C5a: insights from a novel label-free cellular assay. *J. Immunol.* **189**, 4797-4805. doi:10.4049/jimmunol.1200834

Sadeghi, H. and Birnbaumer, M. (1999). O-Glycosylation of the V2 vasopressin receptor. *Glycobiology* **9**, 731-737. doi:10.1093/glycob/9.7.731

Scurci, I., Akondi, K. B., Pinheiro, I., Paolini-Bertrand, M., Borgeat, A., Cerini, F. and Hartley, O. (2021). CCR5 tyrosine sulfation heterogeneity generates cell surface receptor subpopulations with different ligand binding properties. *Biochim. Biophys. Acta Gen. Subj.* **1865**, 129753. doi:10.1016/j.bbagen.2020.129753

Seibert, C., Veldkamp, C. T., Peterson, F. C., Chait, B. T., Volkman, B. F. and Sakmar, T. P. (2008). Sequential tyrosine sulfation of CXCR4 by tyrosylprotein sulfotransferases. *Biochemistry* **47**, 11251-11262. doi:10.1021/bi800965m

Stone, M. J., Hayward, J. A., Huang, C., Huma, Z. and Sanchez, J. (2017). Mechanisms of regulation of the chemokine-receptor network. *Int. J. Mol. Sci.* **18**, 342. doi:10.3390/ijms18020342

Suply, T., Hannedouche, S., Carte, N., Li, J., Grosshans, B., Schaefer, M., Raad, L., Beck, V., Vidal, S., Hiou-Feige, A. et al. (2017). A natural ligand for the orphan receptor GPR15 modulates lymphocyte recruitment to epithelia. *Sci. Signal.* **10**, eaal0180. doi:10.1126/scisignal.aal0180

Szpakowska, M., Fievez, V., Arumugan, K., van Nuland, N., Schmit, J. C. and Chevigne, A. (2012). Function, diversity and therapeutic potential of the N-terminal domain of human chemokine receptors. *Biochem. Pharmacol.* **84**, 1366-1380. doi:10.1016/j.bcp.2012.08.008

Tan, J. H., Ludeman, J. P., Wedderburn, J., Canals, M., Hall, P., Butler, S. J., Taleski, D., Christopoulos, A., Hickey, M. J., Payne, R. J. et al. (2013). Tyrosine sulfation of chemokine receptor CCR2 enhances interactions with both monomeric and dimeric forms of the chemokine monocyte chemoattractant protein-1 (MCP-1). *J. Biol. Chem.* **288**, 10024-10034. doi:10.1074/jbc.M112.447359

Veldkamp, C. T., Seibert, C., Peterson, F. C., De la Cruz, N. B., Haugner, J. C., Basnet, H., Sakmar, T. P. and Volkman, B. F. (2008). Structural basis of CXCR4 sulfotyrosine recognition by the chemokine SDF-1/CXCL12. *Sci. Signal.*. **1**, ra4.

Villanueva-Cabello, T. M., Mollicone, R., Cruz-Munoz, M. E., Lopez-Guerrero, D. V. and Martinez-Duncker, I. (2015). Activation of human naive Th cells increases surface expression of GD3 and induces neoexpression of GD2 that colocalize with TCR clusters. *Glycobiology* **25**, 1454-1464. doi:10.1093/glycob/cwv062

Wang, X., Pan, B., Honda, G., Wang, X., Hashimoto, Y., Ohkawara, H., Xu, K., Zeng, L. and Ikezoe, T. (2018). Cytoprotective and pro-angiogenic functions of thrombomodulin are preserved in the C loop of the fifth epidermal growth factor-like domain. *Haematologica* **103**, 1730-1740. doi:10.3324/haematol.2017.184481

Xu, J., Deng, X., Tang, M., Li, L., Xiao, L., Yang, L., Zhong, J., Bode, A. M., Dong, Z., Tao, Y. et al. (2013). Tyrosylprotein sulfotransferase-1 and tyrosine sulfation of chemokine receptor 4 are induced by Epstein-Barr virus encoded latent membrane protein 1 and associated with the metastatic potential of human nasopharyngeal carcinoma. *PLoS ONE* **8**, e56114. doi:10.1371/journal.pone.0056114

Yang, M., Tang, M., Ma, X., Yang, L., He, J., Peng, X., Guo, G., Zhou, L., Luo, N., Yuan, Z. et al. (2015). AP-57/C10orf99 is a new type of multifunctional antimicrobial peptide. *Biochem. Biophys. Res. Commun.* **457**, 347-352. doi:10.1016/j.bbrc.2014.12.115

Zhu, J. Z., Millard, C. J., Ludeman, J. P., Simpson, L. S., Clayton, D. J., Payne, R. J., Widlanski, T. S. and Stone, M. J. (2011). Tyrosine sulfation influences the chemokine binding selectivity of peptides derived from chemokine receptor CCR3. *Biochemistry* **50**, 1524-1534. doi:10.1021/bi101240v

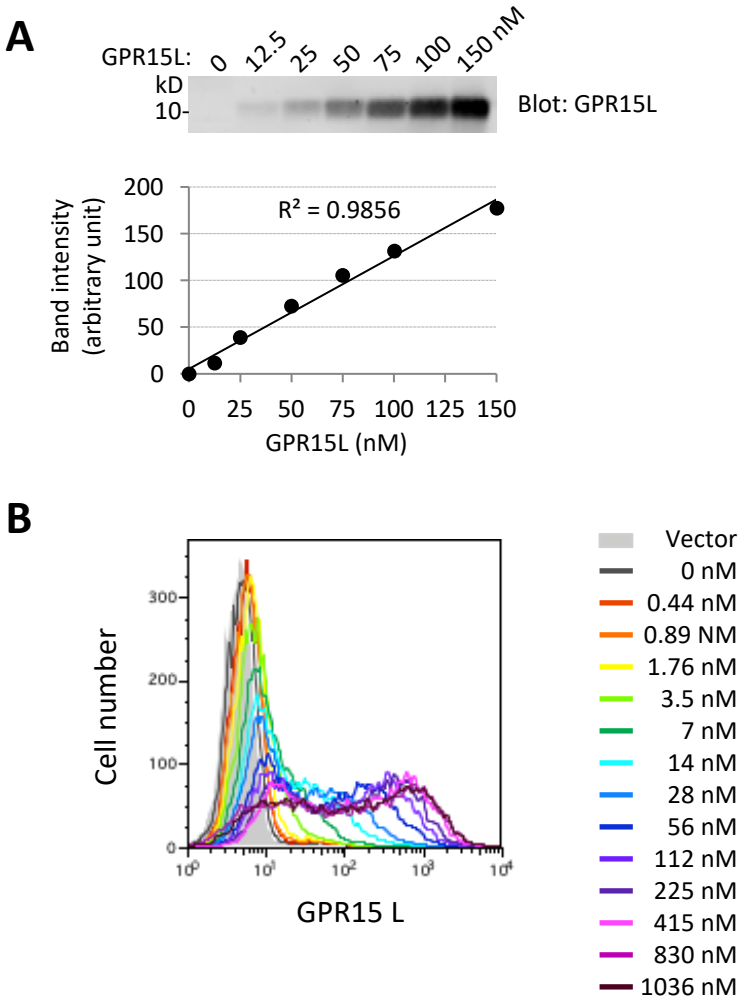

Figure S1. **A**. **Dose-signal relationship of GPR15L blot**. Indicated doses of synthetic full-length GPR15L peptide (aa 1-57) were resolved on 10% SDS-PAGE and immunoblotted with anti-GPR15L Ab (upper panel). Blot was analyzed by near-infrared fluorescence to generate a standard curve (lower panel), which was used to quantify FLAG-GPR15L in the culture supernatants or purified proteins. **B**. **Dose-dependent binding of FLAG-GPR15L to GPR15 receptor**. HEK293 cells transfected with control plasmid (Vector) or untagged GPR15 were incubated with indicated concentrations of purified FLAG-GPR15L followed by staining with PE-labeled anti-FLAG Ab. Histograms from FCM analysis were overlaid.

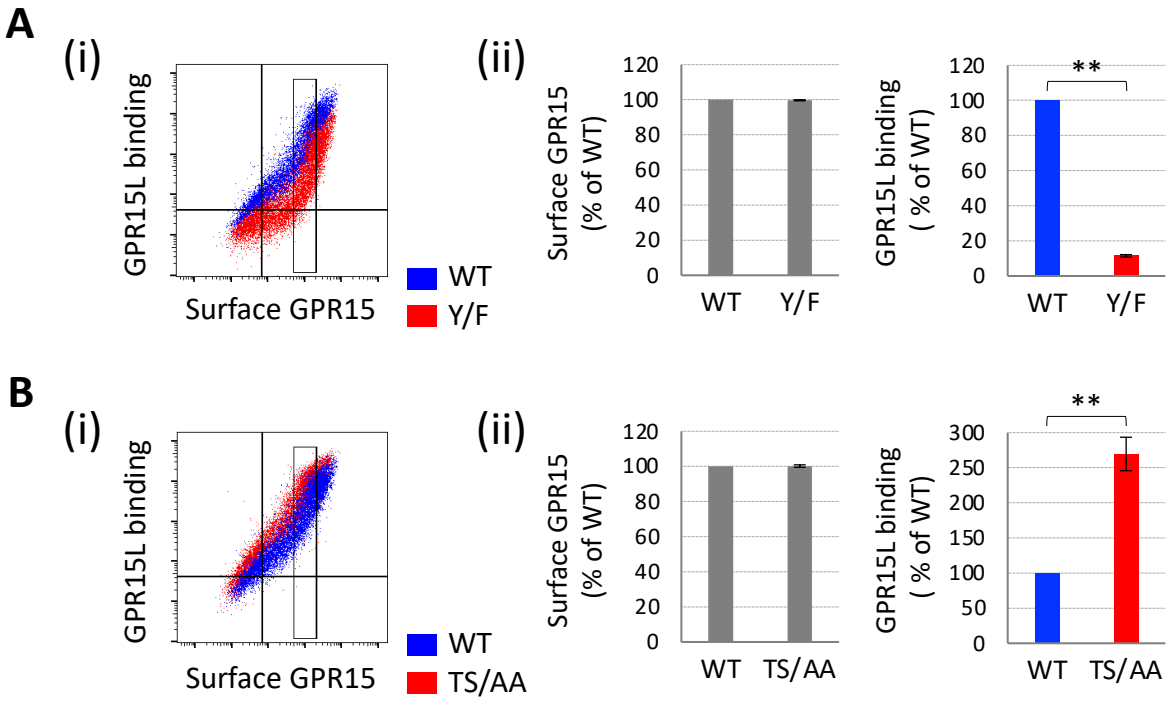

Figure S2. Effects of Y/F and TS/AA mutations of untagged GPR15 receptor on the ligand binding. HEK293 cells transfected with GPR15 WT or Y/F mutant (**A**) or TS/AA mutant (**B**) were incubated with FLAG-GPR15L-containing supernatant and then double stained with BV421-GPR15 Ab and PE-FLAG Ab to quantify surface GPR15 expression and the bound GPR15L, respectively. Shown in (i) are the representative dot plots of double-stained cells in which the thresholds of GPR15 and FLAG signals are indicated by black lines. The gated cell populations (black square) were quantified for surface GPR15 expression (ii, left panel) and FLAG-GPR15L binding (ii, right panel). Statistically significant differences are indicated by (**) ($p \leq 0.01$).

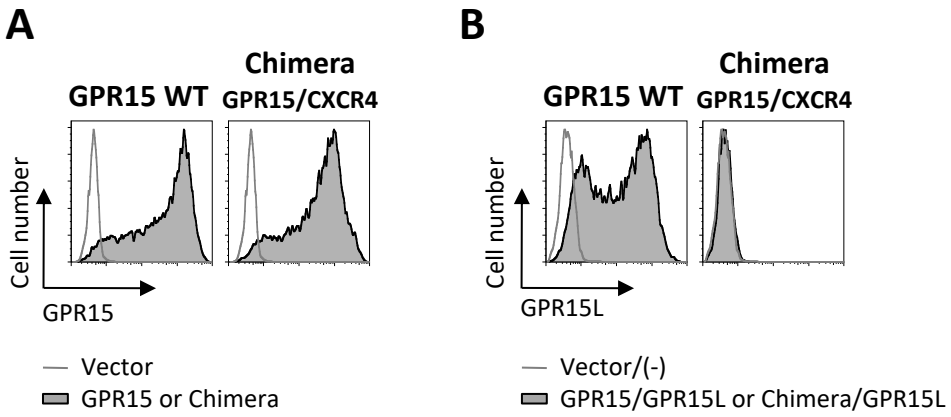

Figure S3. N-terminal tail of GPR15 alone is not sufficient for supporting GPR15L binding. A. Untagged GPR15 or chimeric CXCR4 with N-terminal tail of untagged GPR15 was expressed in HEK293 cell and stained with anti-GPR15 Ab. **B**. Same cells were subjected to FLAG-GPR15L binding assay and stained with anti-FLAG Ab.

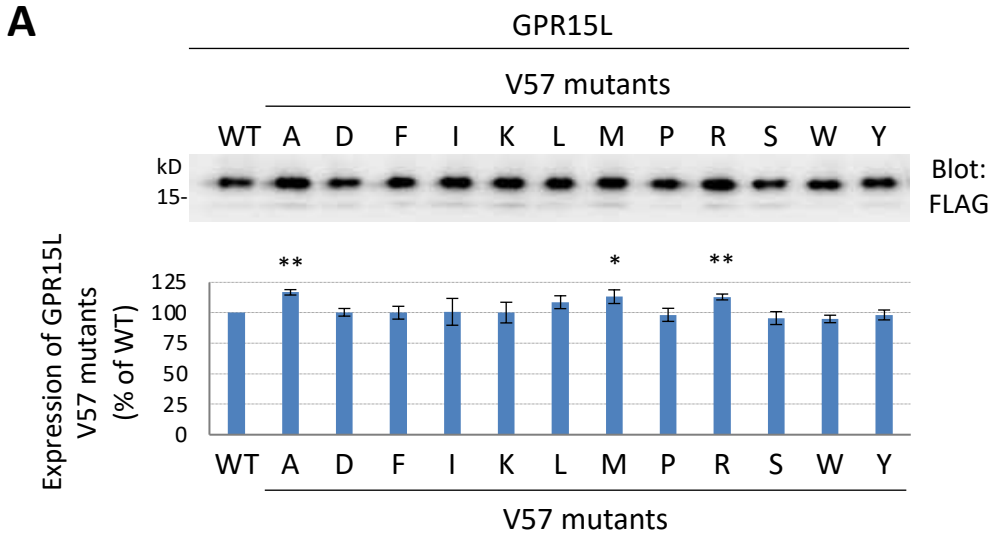

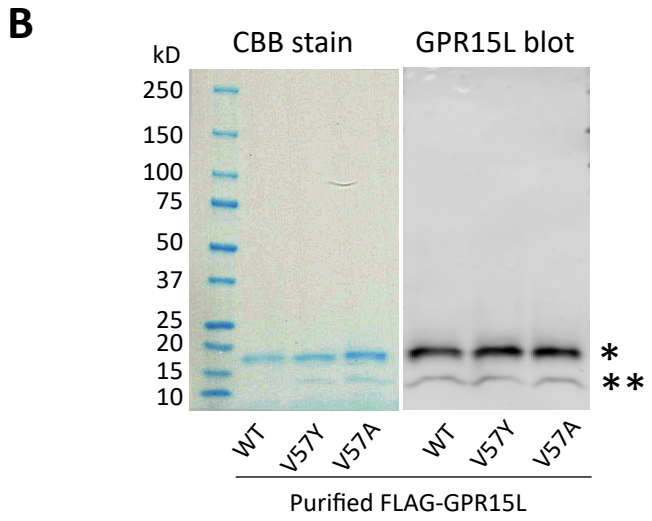

Figure S4. A. Relative expression level of FLAG-GPR15L proteins with mutations in C-terminal Val[57]. Culture supernatants from FLAG-GPR15L transfected HEK293T cells were immunoblotted for FLAG (upper panel) and the relative band intensities to the WT protein were determined by quantitation using fluorescence imaging (lower panel). Data points represent mean ± SEM of triplicate samples from a representative experiment. Statistically significant differences are indicated by * ($p \leq 0.05$) and ** ($p \leq 0.01$). **B. Purity of isolated FLAG-GPR15 proteins**. FLAG-GPR15 proteins (WT, V57Y, V57A) purified from culture supernatants of transfected HEK293T cells were resolved on 4-15% SDS-PAGE and then visualized by Coomassie Brilliant Blue stain (left) or immunoblot with GPR15L Ab (right). The difference in the migration of the two bands (* and **) is related to glycosylation (unpublished data).